THE TRANSMISSION-LINE PARADIGM FOR METAMATERIALS: FUNDAMENTALS & SELECTED APPLICATIONS

George V. Eleftheriades

The Edward S. Rogers Sr. Department of Electrical and Computer Engineering
The University of Toronto
CANADA

METAMATERIALS

META="BEYOND" IN GREEK

Artificial materials with unusual electromagnetic properties that are difficult to encounter in nature.

ARTIFICIAL DIELECTRICS:

- W.E. Kock "Metallic delay lenses", Bell Syst. Tech. J., vol. 27, pp. 58-82, Jan. 1948.
- R.N. Bracewell, "Analogues of an ionized medum", Wireless Eng. Dec. 1954.
- S.B. Cohn, "The electric and magnetic constants of metallic delay media containing obstacles of arbitrary shape and thickness," Journal of Applied Physics, vol. 22, May, 1951.
- W. Rotman, "Plasma simulation by artificial dielectrics and parallel-plate media", IRE Trans. on Antennas and Propagation, Jan. 1962.
- R. E. Collin, *Field Theory of Guided Waves*, Piscataway, N.J.: IEEE Press, 1990 (chapter 12).

TRANSMISSION-LINE METAMATERIALS:

Artificial dielectrics synthesized by periodically loading a host transmission-line medium with R,L,C lumped elements: Periodicity $<<\lambda$ (although non-periodic MTMs could also be defined).

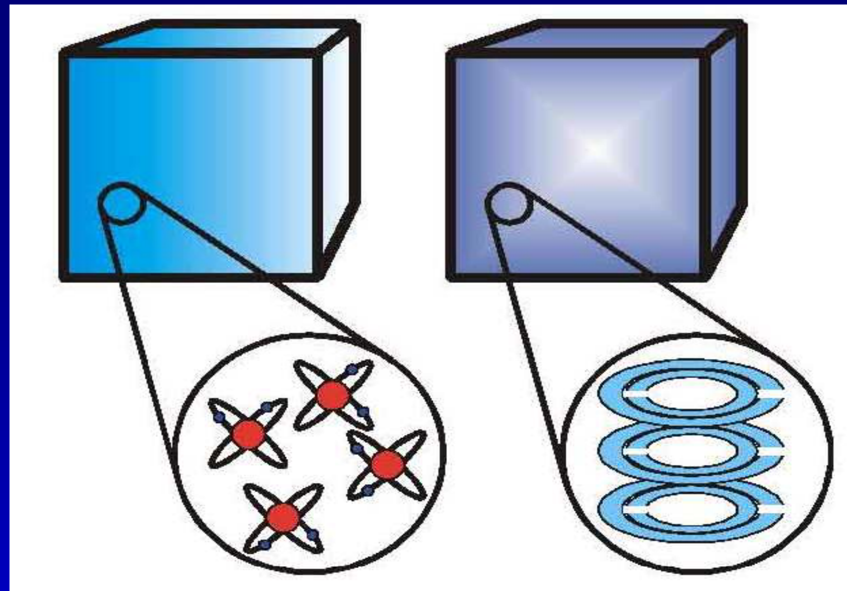

J.B. Pendry

Artificial Molecules

1948

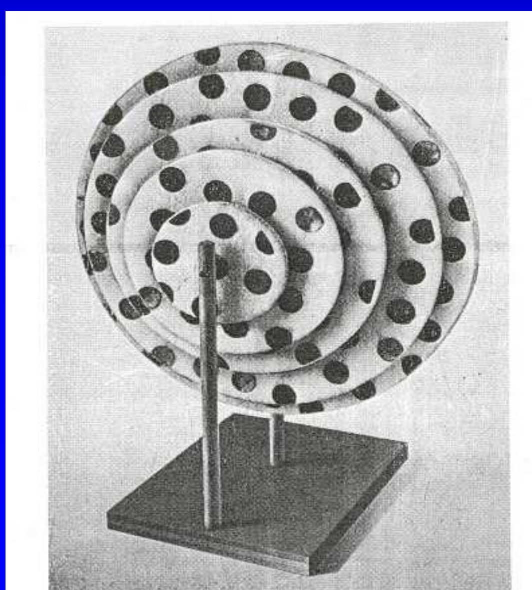

2001

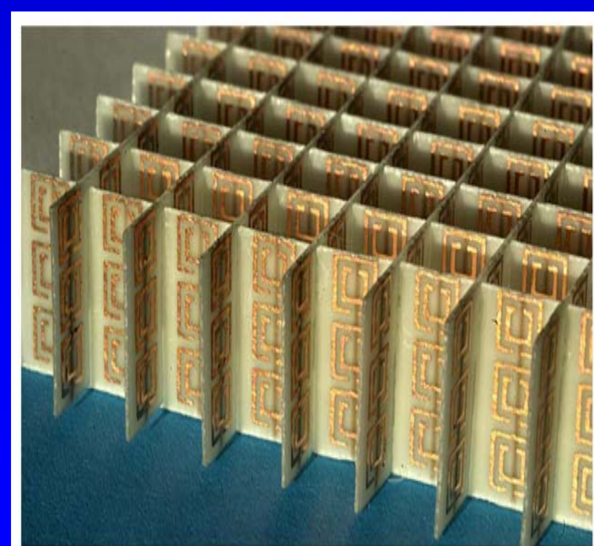

2008

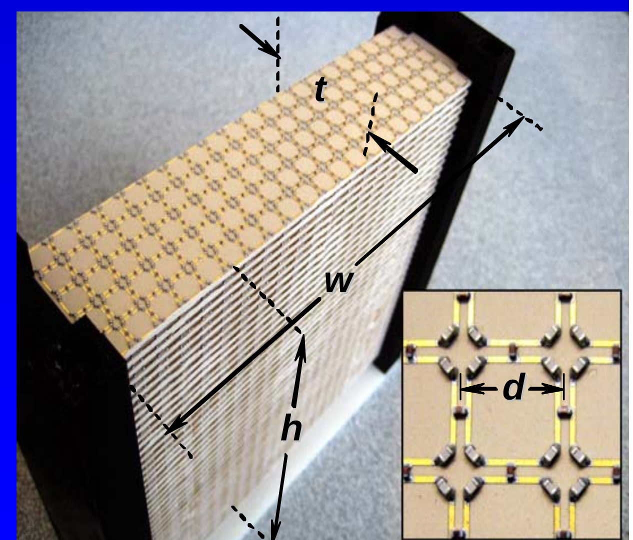

FUNDAMENTALS

LEFT-HANDED ε<0 AND μ<0 METAMATERIALS

Veselago, 1960s

Backward Waves

$\varepsilon > 0, \mu > 0$

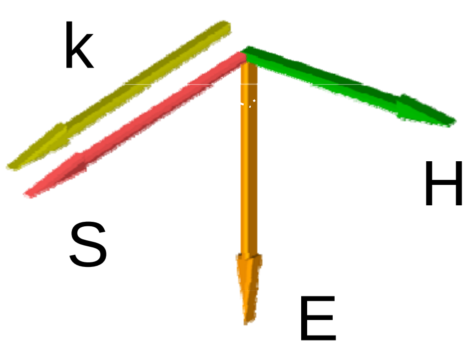

Regular Materials

(right-handed)

$\varepsilon < 0, \mu < 0$

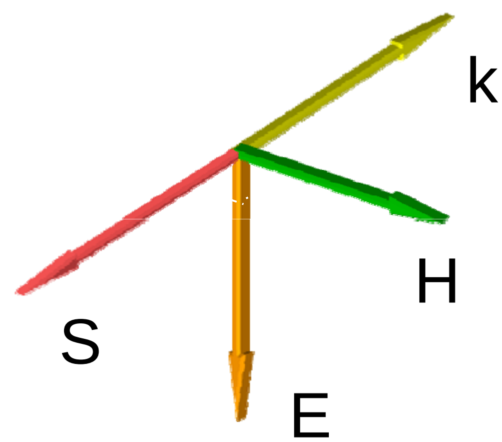

Left-handed Materials

$n = -\sqrt{\varepsilon\mu}$

Negative-Refractive-Index (NRI) Materials

NEGATIVE REFRACTION

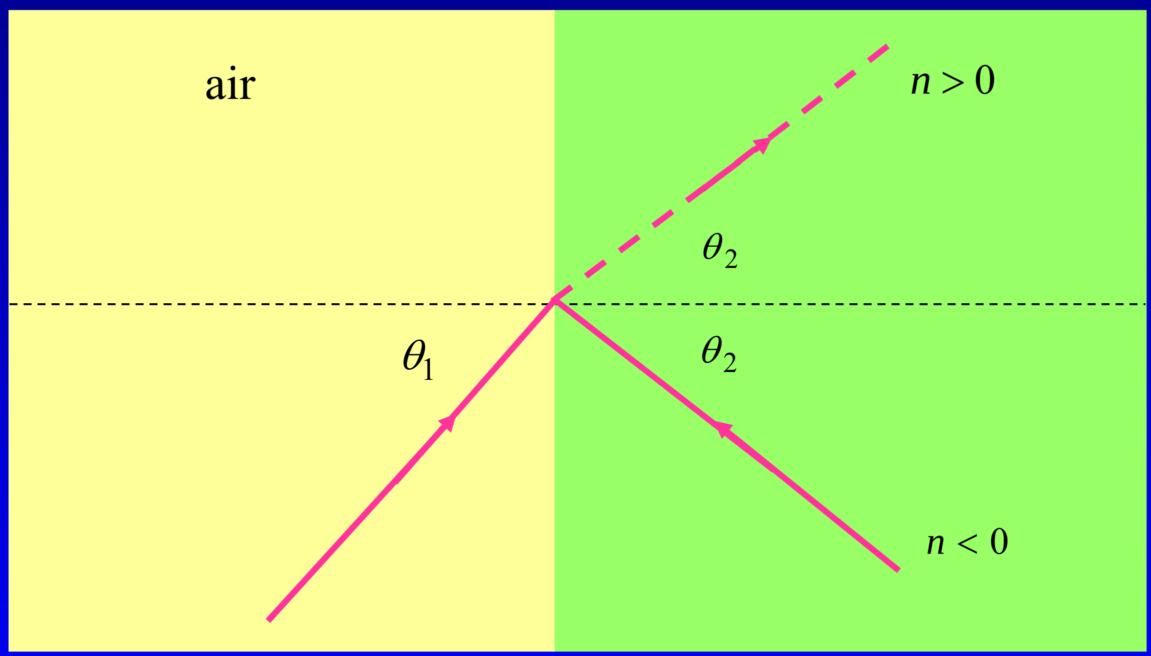

$$\frac{\sin\theta_1}{\sin\theta_2} = n$$

Negative-Refractive-Index (NRI) Media

RECONCEPTUALIZING ε<0 AND μ<0 METAMATERIALS

Start from the transmission-line representation of normal dielectrics:

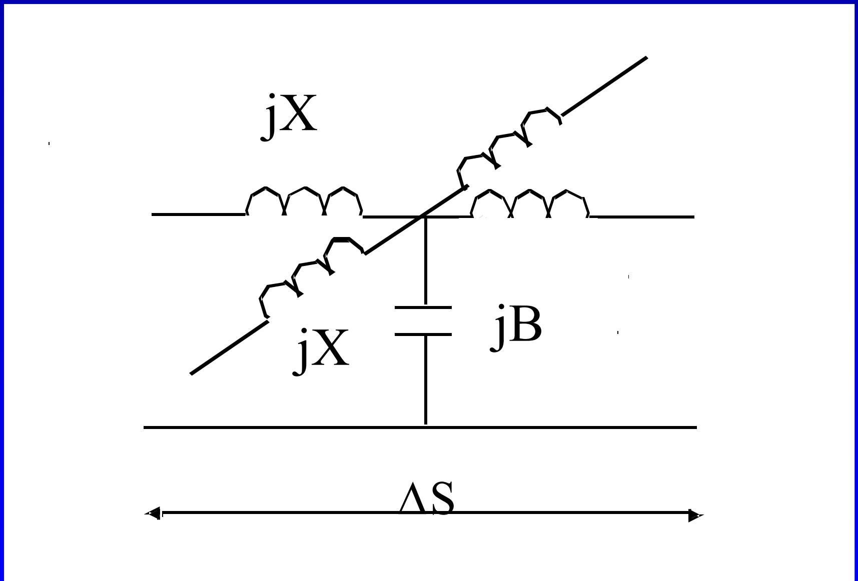

$$j\omega\mu = \frac{jX}{\Delta S} = \frac{j\omega L}{\Delta S} \Rightarrow \mu = \frac{L}{\Delta S}$$

$$j\omega\varepsilon = \frac{jB}{\Delta S} = \frac{j\omega C}{\Delta S} \Rightarrow \varepsilon = \frac{C}{\Delta S}$$

How to synthesize ε<0, μ<0?

Simply: Make the series reactance X and shunt susceptance B both negative!

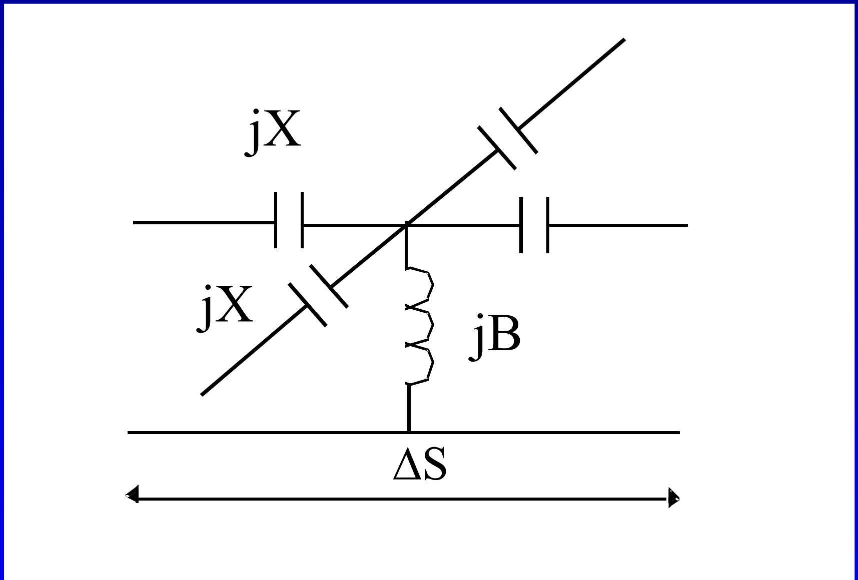

$$j\omega\varepsilon = \frac{jB}{\Delta S} = \frac{j(-1/\omega L)}{\Delta S} \Rightarrow \varepsilon = -\frac{1}{\omega^2 L \Delta S}$$

$$j\omega\mu = \frac{jX}{\Delta S} = \frac{j(-1/\omega C)}{\Delta S} \Rightarrow \mu = -\frac{1}{\omega^2 C \Delta S}$$

G.V. Eleftheriades, A.K. Iyer and P.C. Kremer, "Planar negative refractive index media using periodically L-C loaded transmission lines," ***IEEE Trans. on Microwave Theory and Techniques,*** **vol. 50, no. 12, pp. 2702-2712, Dec. 2002.**

L. Liu, C. Caloz, C. Chang, T. Itoh, "Forward coupling phenomenon between artificial left-handed transmission lines," ***J. Appl. Phys.*****, vol. 92, no. 9 , pp. 5560-5565, 2002.**

Planar Negative Refractive Index Media Using Periodically L–C Loaded Transmission Lines

George V. Eleftheriades, *Senior Member, IEEE,* Ashwin K. Iyer, *Student Member, IEEE*, and Peter C. Kremer

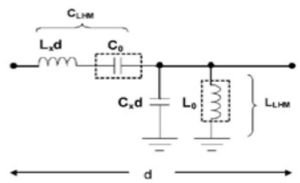

Fig. 6: 1-D unit cell with host transmission line medium embedded as an equivalent series inductor and shunt capacitor.

sary to develop a procedure to modify the values of the discrete loading elements such that the value of β is restored, particularly at the frequency of operation, to that obtained in the dimensionless case. That is, the key design idea is to explicitly account for the contribution of the transmission-line parameters in the total inductance and capacitance per unit cell. Specifically, the per-unit-length transmission line parameters of the line L_x and C_x can be incorporated into the unit cell by modifying the cell as depicted for the 1-D case in Fig. 6.

Here, C_0 and L_0 are the new loading elements, and the total impedance in the series and shunt branches give the designed equivalent series capacitance C_{LHM} and shunt inductance L_{LHM}, respectively, at the design frequency.

The required new series loading capacitance C_0 can be determined using the following equation,

$$j\omega L_x d + \frac{1}{j\omega C_0} = \frac{1}{j\omega C_{LHM}}, \tag{30}$$

which simplifies, through some manipulation, to the desired result

$$C_0 = \frac{C_{LHM}}{1+\omega^2 C_{LHM} L_x d}. \tag{31}$$

Before specifying L_0, it is important to note that, in the 2-D version of the medium, it is necessary to further compensate for the effect of the host medium transverse to the direction of propagation. This is most clearly illustrated for the case of normal incidence, for which each of the two transverse transmission line segments become open-circuited at their centres, and, therefore, contribute capacitively to the unit cell. This is shown in Fig. 7 from the top-view. Consequently,

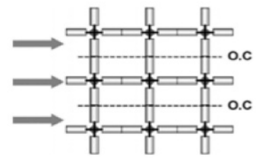

Fig. 7: Top view of transmission line grid, showing open-circuits formed in the medium transverse to the direction of propagation, for the case of normal incidence.

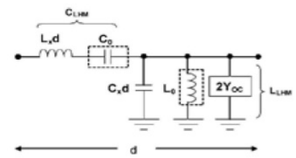

Fig. 8: The one-dimensional unit cell of Fig. 6 with the effect of the transverse host medium represented as a shunt capacitance Y_{OC}.

through the use of the small angle approximation. That is, for kd<<2, the third term on the left-hand side of (32) becomes identical to the first term. It is, therefore, apparent that the capacitive contribution of the two open-circuited stubs in shunt is limited to the effect of their transmission line parameters. Moreover, since C_x can be given by $\varepsilon_r\varepsilon_0$, the transverse stubs serve, effectively, to double the relative permittivity of the unloaded medium if they are not compensated for.

The equivalent material parameters of (12) and (13) may now be given by

$$\mu_S = \mu_{r,LHM}\mu_0 = -\frac{1}{\omega^2 C_{LHM} d} = L_x - \frac{1}{\omega^2 C_0 d} \tag{34}$$

$$\varepsilon_S = \varepsilon_{r,LHM}\varepsilon_0 = -\frac{1}{\omega^2 L_{LHM} d} = 2C_x - \frac{1}{\omega^2 L_0 d} \tag{35}$$

from which it can be seen that each of these parameters consists of a positive contribution due to the unloaded medium, and a negative contribution due to the loading (corresponding to an effective negative susceptibility).

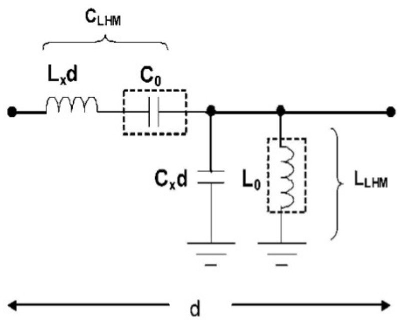

Fig. 6: 1-D unit cell with host transmission line medium embedded as an equivalent series inductor and shunt capacitor.

sary to develop a procedure to modify the values of the discrete loading elements such that the value of β is restored, particularly at the frequency of operation, to that obtained in the dimensionless case. That is, the key design idea is to explicitly account for the contribution of the transmission-line parameters in the total inductance and capacitance per unit cell. Specifically, the per-unit-length transmission line parameters of the line L_x and C_x can be incorporated into the unit cell by modifying the cell as depicted for the 1-D case in Fig. 6.

Here, C_0 and L_0 are the new loading elements, and the total impedance in the series and shunt branches give the designed equivalent series capacitance C_{LHM} and shunt inductance L_{LHM}, respectively, at the design frequency.

The required new series loading capacitance C_0 can be determined using the following equation,

$$j\omega L_x d + \frac{1}{j\omega C_0} = \frac{1}{j\omega C_{LHM}}, \tag{30}$$

Employing a higher level of precision in the approximation of (21) than (22) permits the analytic determination of the stopband limits

$$\cos\beta d \cong 1 - \frac{\theta^2}{2} + \frac{ZY}{2} + \frac{j}{2}\left(\frac{Z}{Z_0} + \frac{Y}{Y_0}\right)\theta. \tag{27}$$

Making the substitutions of (23), with $\theta = kd = \omega d/v$ (where v is the phase velocity in the host medium), and setting $\beta = 0$ in (27), the solution of the resulting quadratic equation in ω yields the desired cut-off frequencies (see Fig. 5) as follows:

$$f_{c,1} = \frac{1}{2\pi}\sqrt{\frac{v}{C_0 Z_0 d}}, \quad f_{c,2} = \frac{1}{2\pi}\sqrt{\frac{v}{L_0 Y_0 d}} \tag{28}$$

Note that both cutoff frequencies in (28) tend to infinity as the cell dimensionality d approaches zero, thus arbitrarily increasing the bandwidth of the first LH passband (see Fig. 5). Furthermore, closing this stopband by equating these two cutoff frequencies yields the matching condition

$$Z_0 = \sqrt{\frac{L_0}{C_0}} \tag{29}$$

which suggests that the width of the stopband may be controlled by adjusting the mismatch between the characteristic impedances of the host medium and the loading. It is clear from the lowest

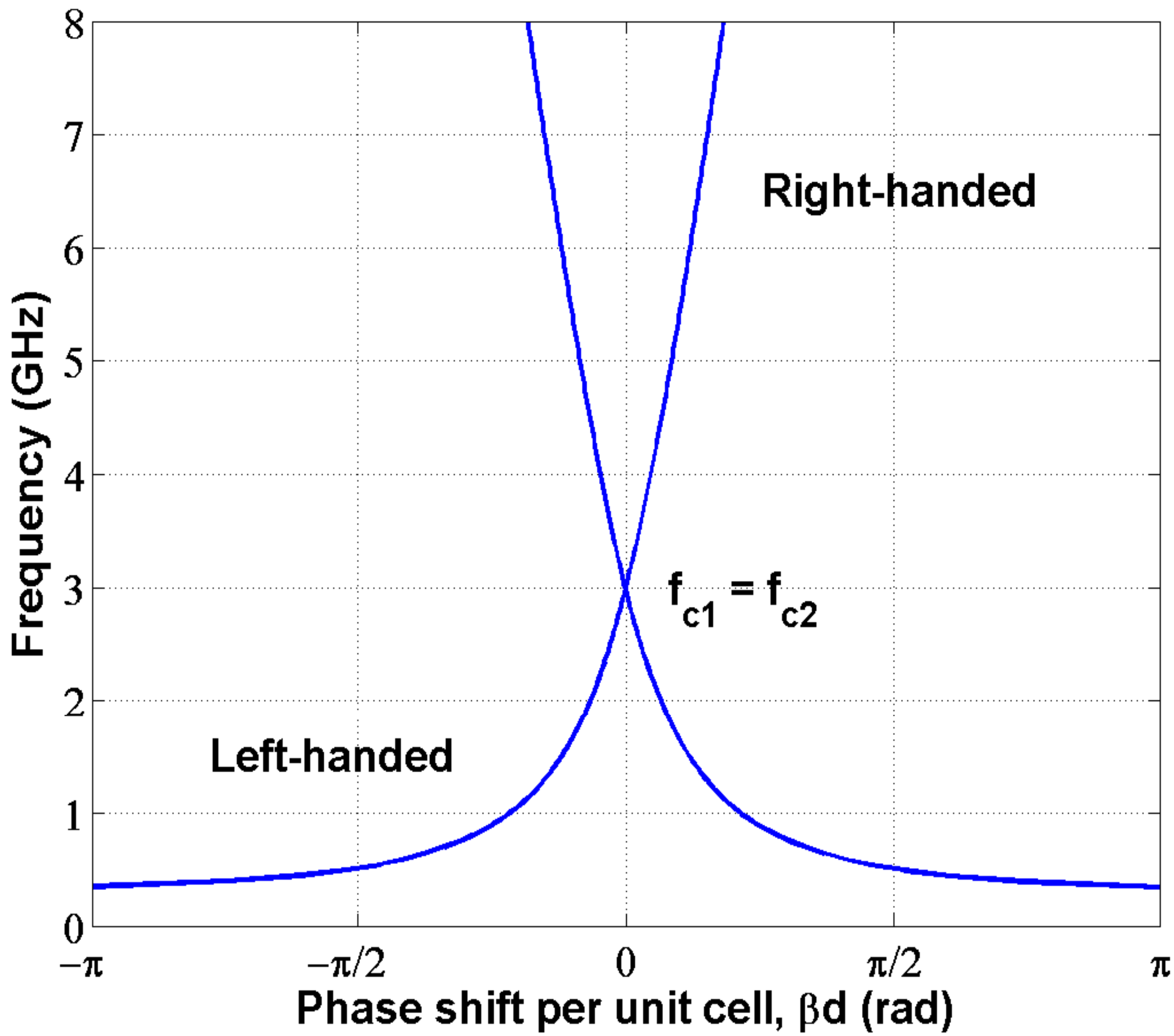
Right-handed
Left-handed
$f_{c1} = f_{c2}$
Frequency (GHz)
Phase shift per unit cell, βd (rad)
0
1
2
3
4
5
6
7
8
−π
−π/2
0
π/2
π

2D Microstrip Implementation of NRI-TL Metamaterials

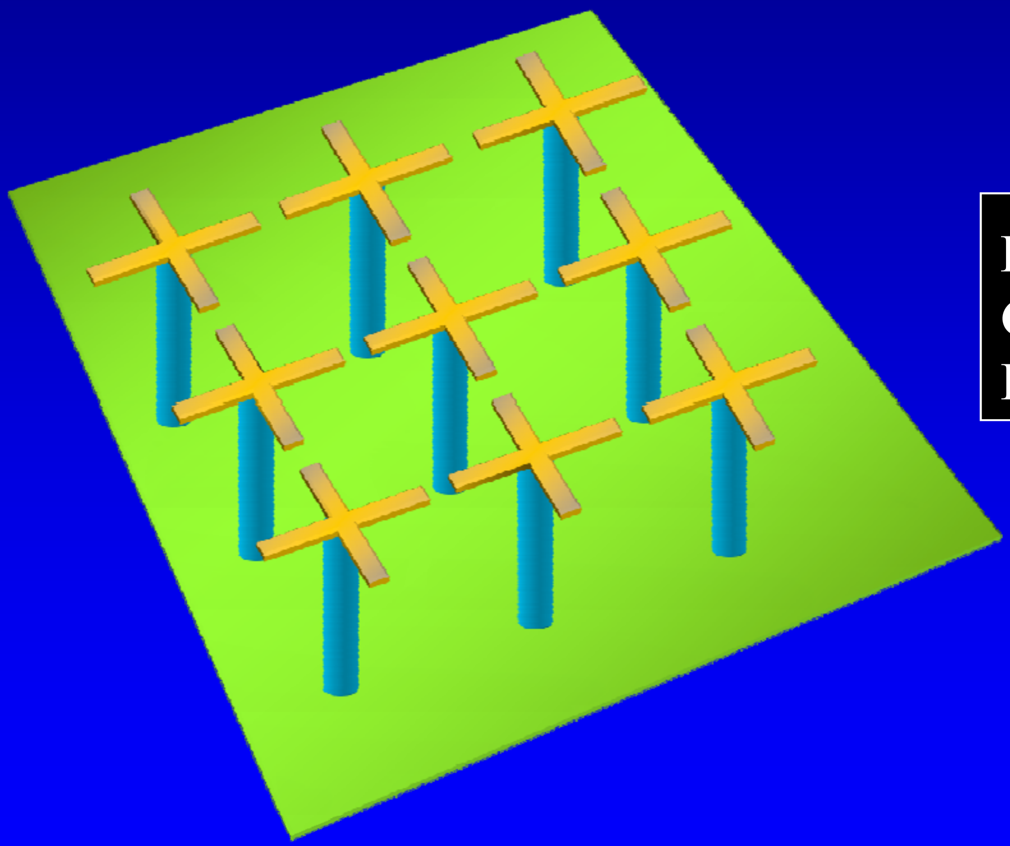

Distributed TL Network With Chip or Printed (gaps and vias) Loading Lumped Elements

IEEE Microwave and Wireless Components Letters vol. 13,no. 4, pp. 155-157, April 2003.

Effective Medium Approach for a Left-Handed Loaded Parallel-Plate Waveguide (PPW)

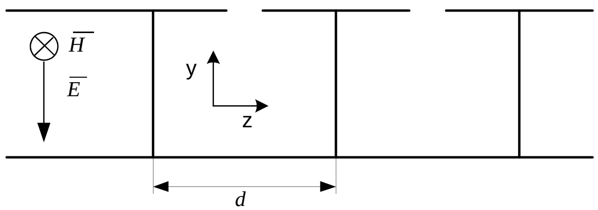

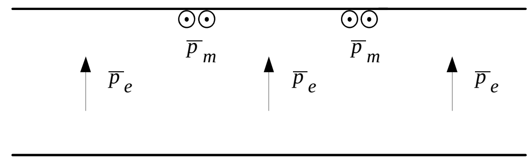

Ampere's Law: $\nabla \times \overline{H} = j\omega\varepsilon_o \overline{E} + j\omega \overline{P}_e$ $\quad \overline{P}_e = -\dfrac{\overline{E}}{\omega^2 L_o d}$ (x-z loop)

Faraday's Law: $\nabla \times \overline{E} = -j\omega\mu_o \overline{H} - j\omega\mu_o \overline{P}_m$ $\quad \overline{P}_m = -\dfrac{\overline{H}}{\mu_o \omega^2 C_o d}$ (y-z loop)

Equivalent PPW filled with effective media parameters

$$\varepsilon_{eff} = \varepsilon_o - 1/(\omega^2 L_o d)$$

$$\mu_{eff} = \mu_o - 1/(\omega^2 C_o d)$$

Negative-Refraction Metamaterials: Fundamental Principles and Applications. Editors G.V. Eleftheriades and K.G. Balmain (John Wiley & Sons and IEEE Press); contributed four chapters. ISBN: 0-471-60146-2, June 2005.

SPATIAL HARMONICS IN NRI-TL

Proc. of the IEEE European Microwave Conference, pp. 504-507, Sept. 29-Oct.1 2009, Rome, Italy.

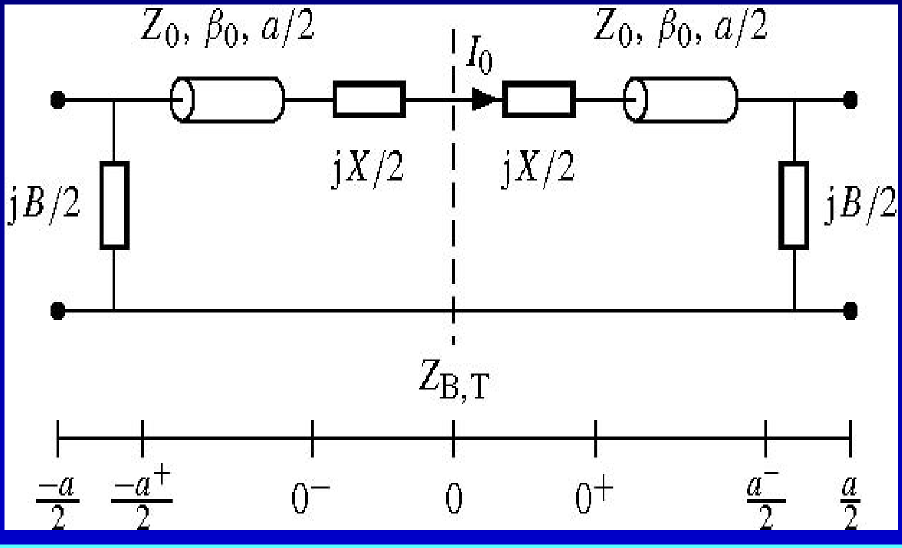

$$V(z) = \sum_{n=-\infty}^{+\infty} u_n e^{-j\beta_n z}$$

$$\beta_n = \beta + \frac{2\pi n}{a}$$

Infinite number of forward $n > 0$
and backward harmonics $n \leq 0$

Just how much power is contained in the fundamental n=0 BW harmonic?

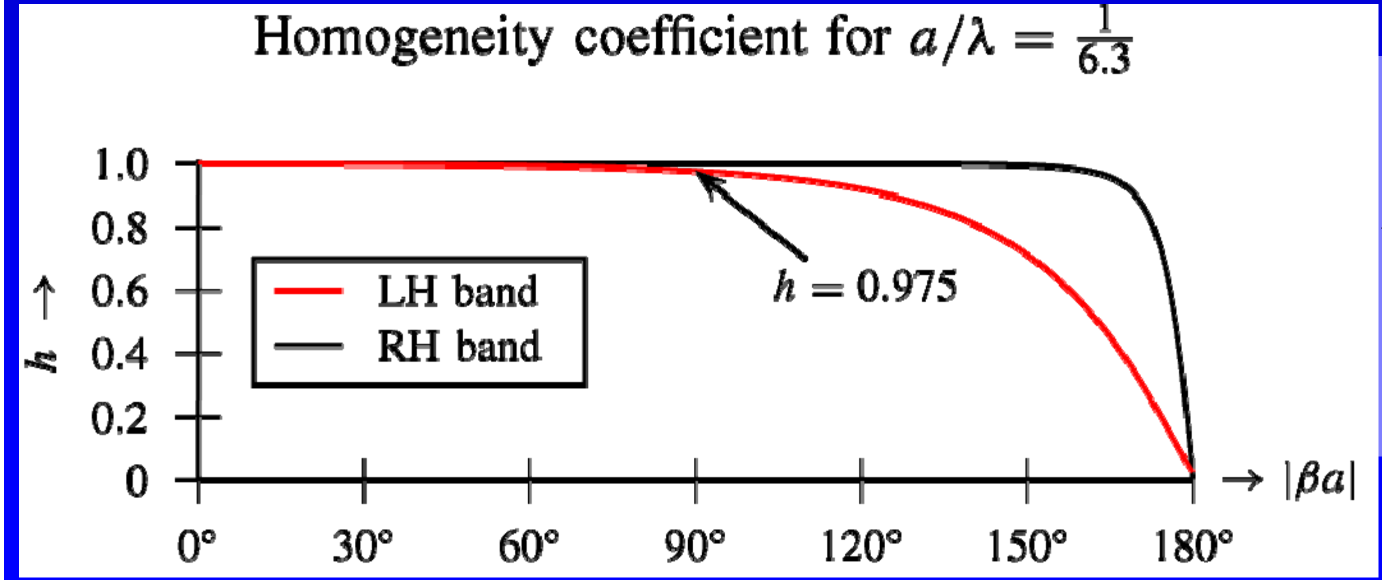

In the homogeneous limit

$\beta a << 1, ka << 1$ most of the power

is carried by the fundamental (n=0) spatial harmonic

PHASE EVOLUTION: How does a Backward Wave Form?

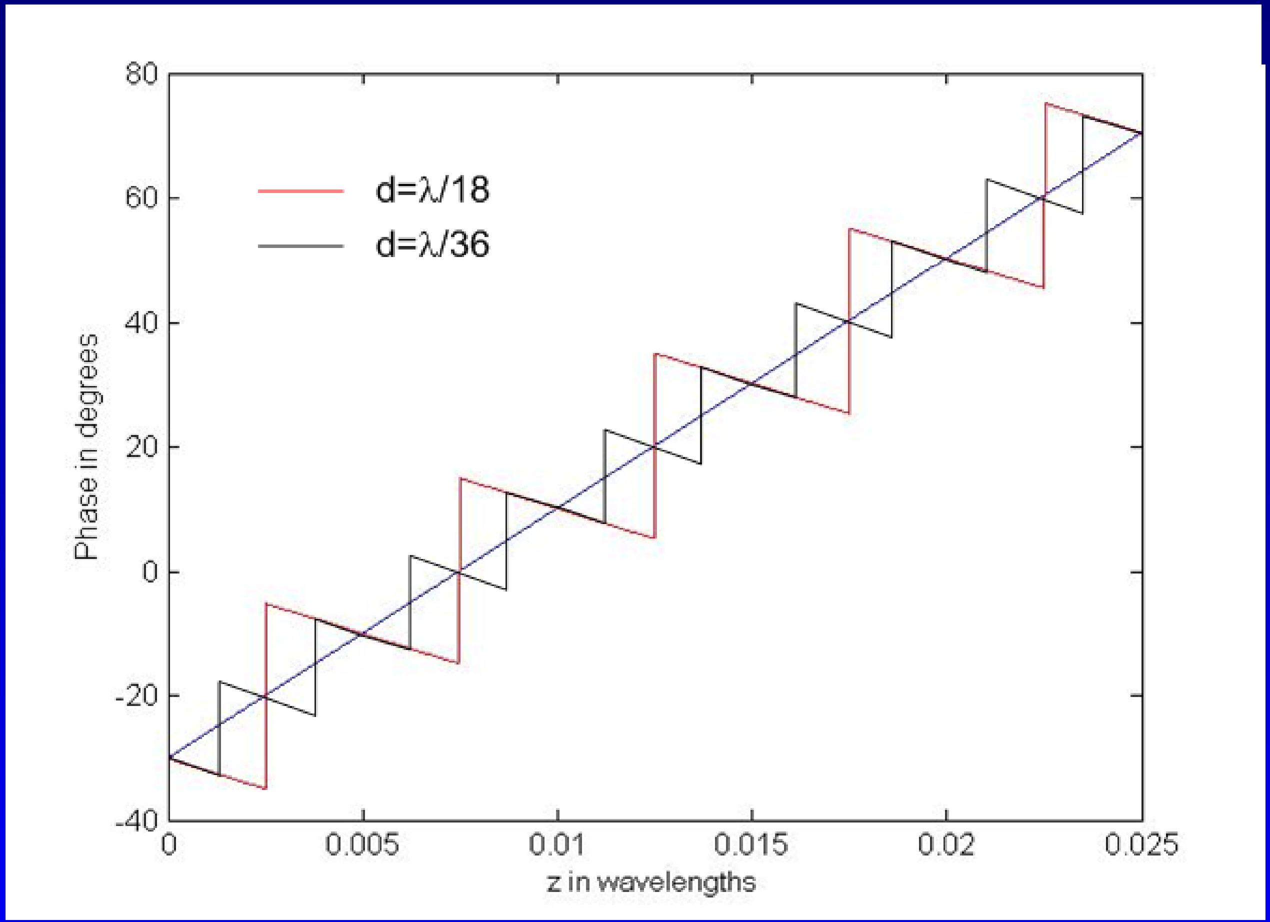

On the interconnecting TL there is a phase delay; the phase advances from one unit cell to the next due to the phase jumps on the shunt inductors (for the current).

On the AVERAGE the phase linearly advances with distance

The departure from the average becomes smaller and smaller as the unit cell becomes smaller

Backward wave on an NRI TL

BROADBAND/LOW-LOSS NATURE OF TL-BASED METAMATERIALS

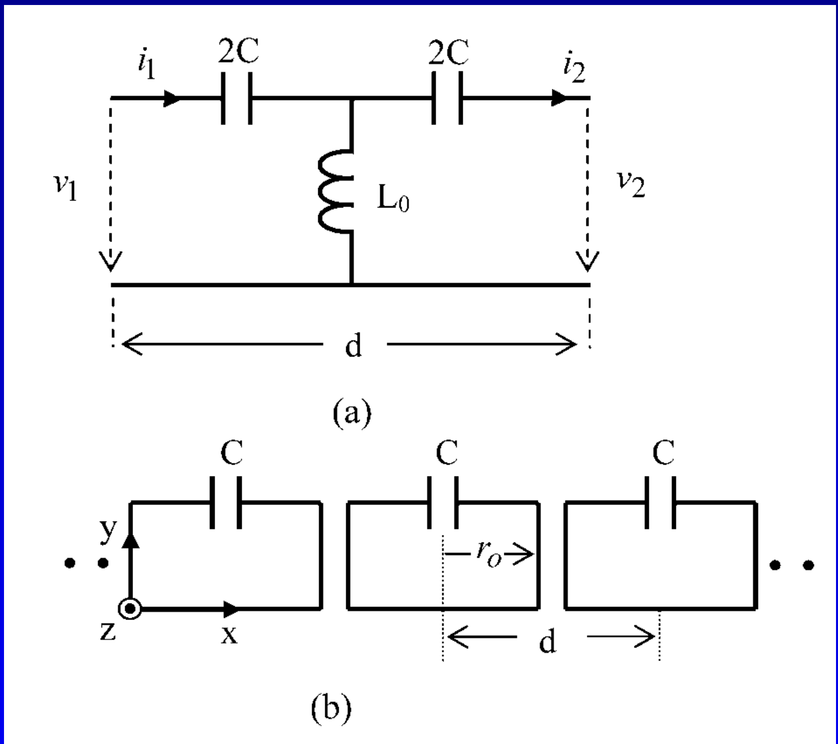

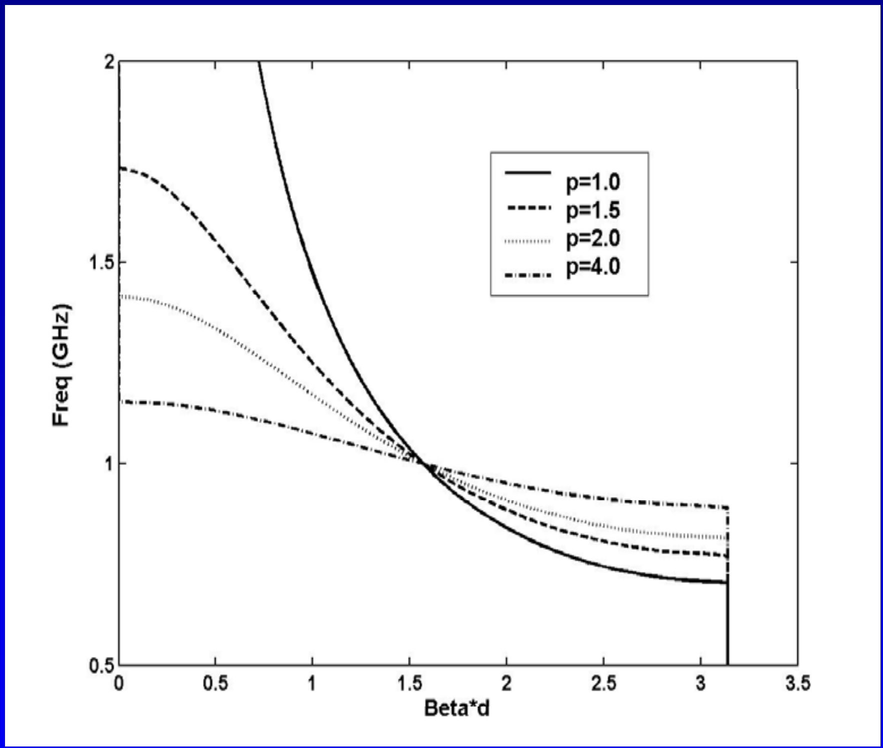

1/p=normalized coupling coefficient between adjacent loops

G.V. Eleftheriades, "Analysis of Bandwidth and Loss in NRI-TL Media Using Coupled Resonators," IEEE Microwave and Wireless Components Letters, June 2007.

NEGATIVE REFRACTION OF A GAUSSIAN BEAM IN NRI-TL METAMATERIALS

Power refracts negatively

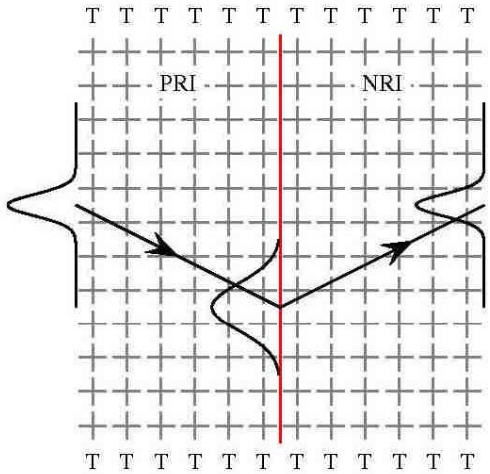

Fig. 6. Schematic auf the Gaussian beam simulation. Grey crosses represent unit cells, on the left hand side a PRI grid is excited by a Gaussian beam, the PRI interfaces a NRI. The Gaussian beam excitation is chosen such that the beam waist forms at the PRI-NRI interface. Towards the side edges the unit cells are terminated by a suitable termination, denoted by 'T'.

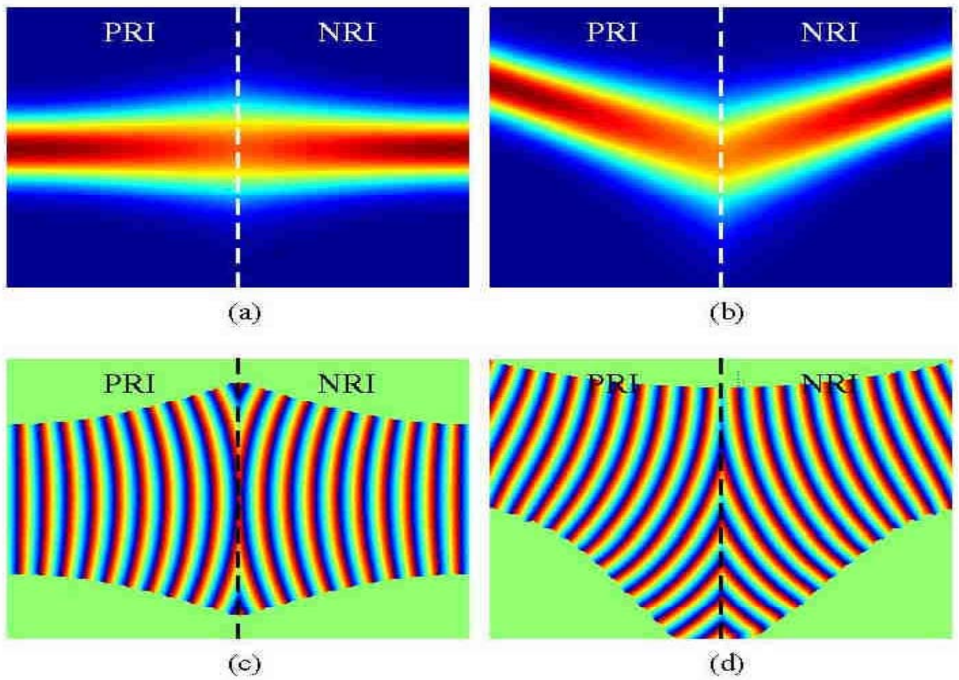

Fig. 7. Simulation results for a Gaussian beam propagating in a grid of 257×340 network unit cells. The left half space is PRI, the right half space is NRI. (a) Linear magnitude plot of a beam at normal incidence. (b) Linear magnitude plot of a beam incident at 20°. (c) Phase plot of the normally incident beam. (d) Phase plot for the beam incident at 20°.

M. Zedler and G.V. Eleftheriades, 2009

1D APPLICATIONS

A LEAKY BACKWARD-WAVE ANTENNA (fan beam)

BACKWARD Radiation from the FUNDAMENTAL Spatial harmonic

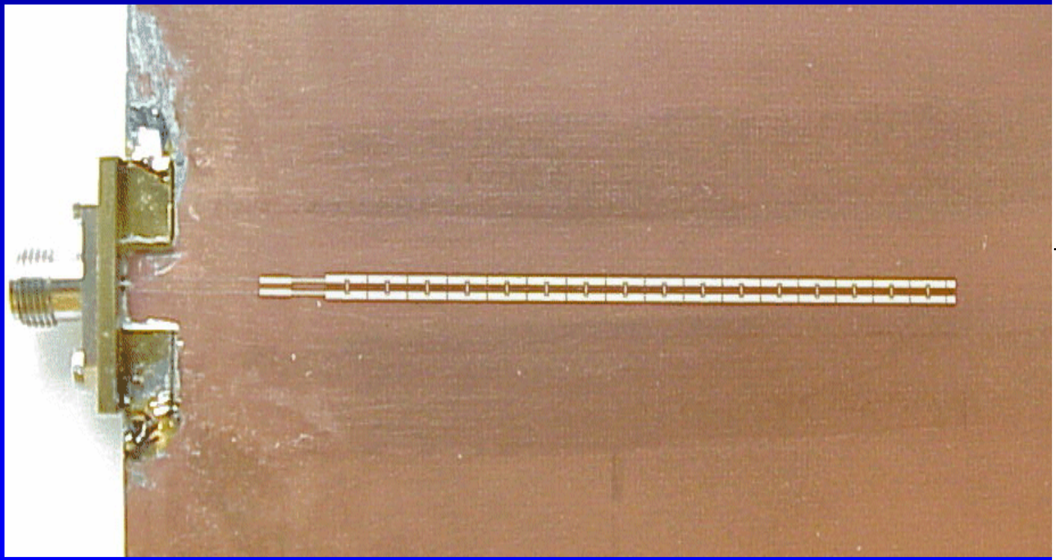

F=15GHz

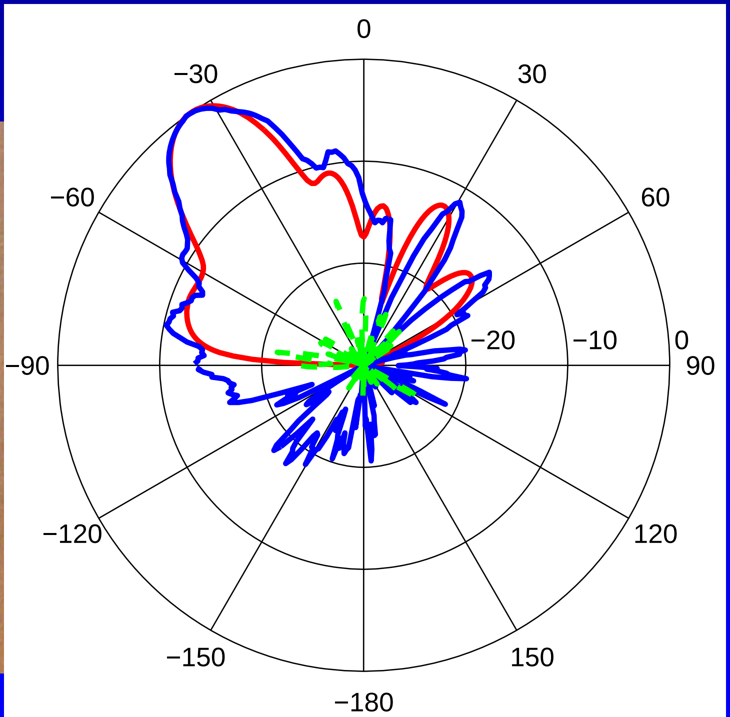

A. Grbic and G.V. Eleftheriades, "Experimental verification of backward-wave radiation from a negative refractive index metamaterial." *Journal of Applied Physics*, vol. 92, pp. 5930-5935, Nov. 2002.

2D NRI-TL Leaky-Wave Antenna

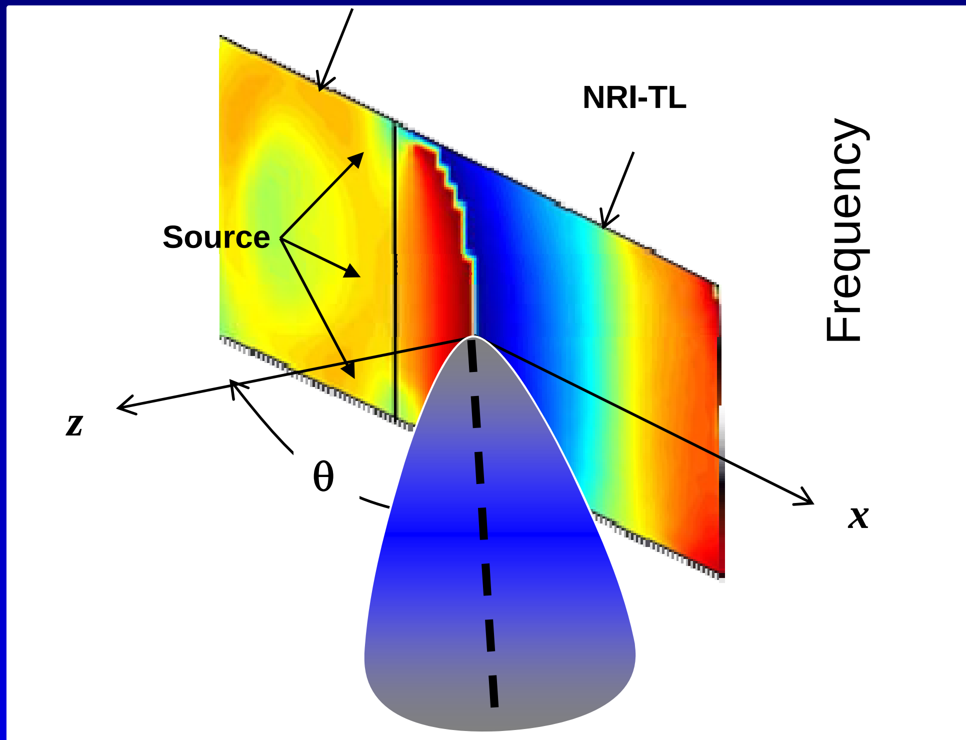

Closed Stop Band

$$\frac{Z_o}{\sqrt{2}} = \sqrt{\frac{L_o}{C_o}}$$

Directivity

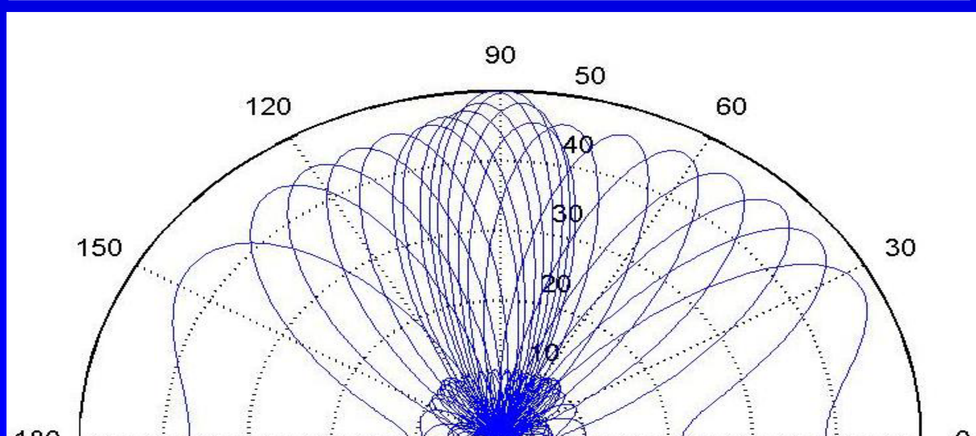

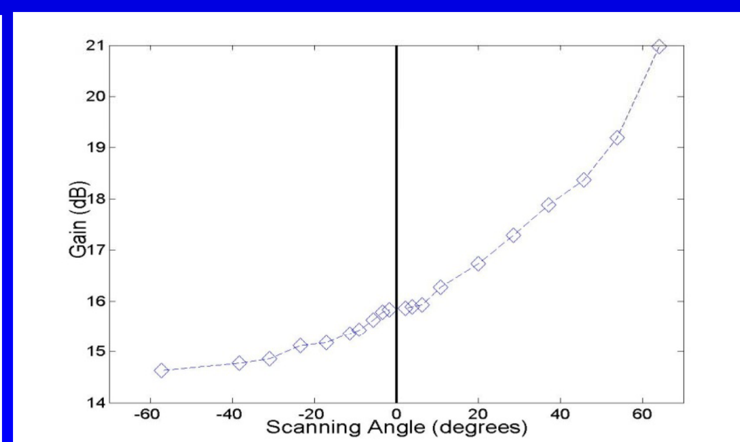

T. Kokkinos, C.D. Sarris and G.V. Eleftheriades, "Periodic FDTD analysis of leaky-wave structures and applications to the analysis of negative-refractive-index leaky-wave antennas," *IEEE Trans. on Microwave Theory Tech.*, May 2006.

REDUCED BEAM-SQUINTING LEAKY-WAVE ANTENNA (in planar CPS)

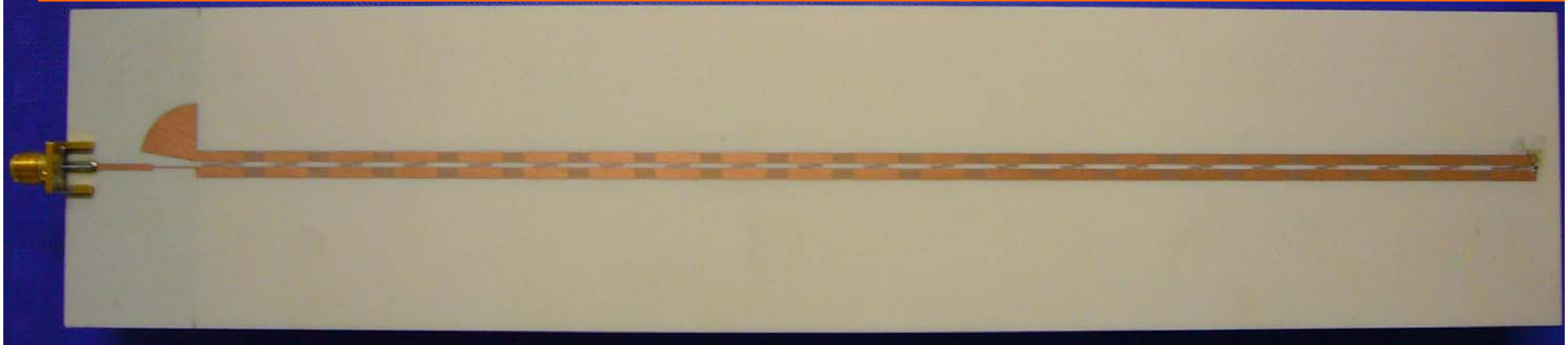

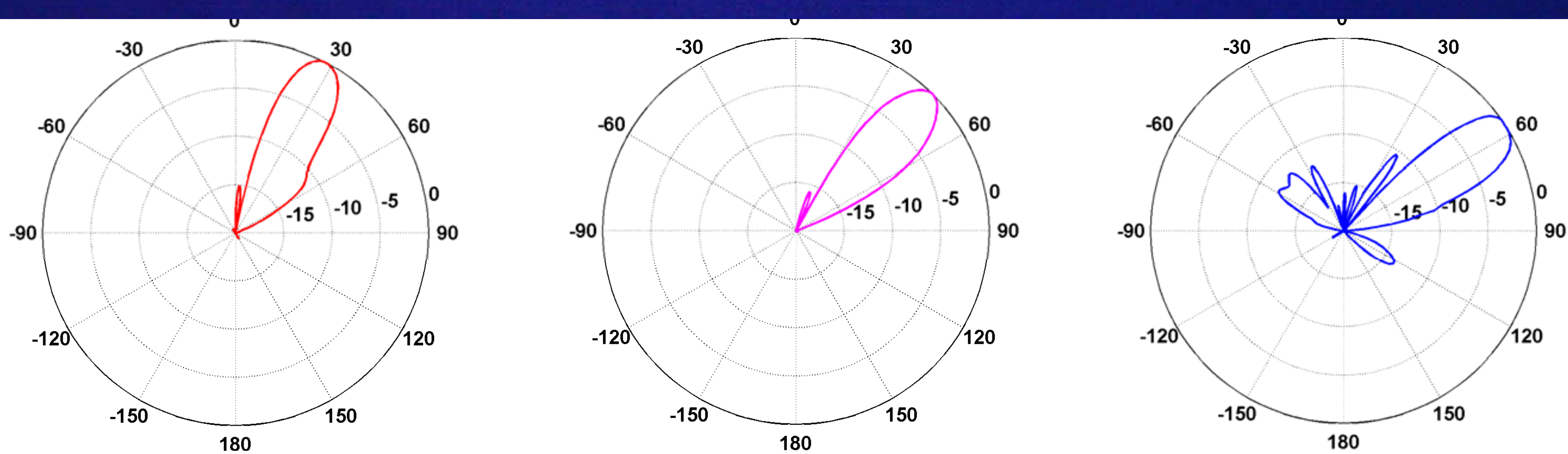

4.5 GHz 5.0 GHz 5.5 GHz

M. Antoniades and G.V. Eleftheriades, IEEE Trans. on Antennas and Propagat., vol. 56, no. 3, pp. 708-721, March 2008.

Zero-Degree Phase-Shifting Lines

Phase Compensation with RHM/LHM Lines

$-\phi$	$+\phi$

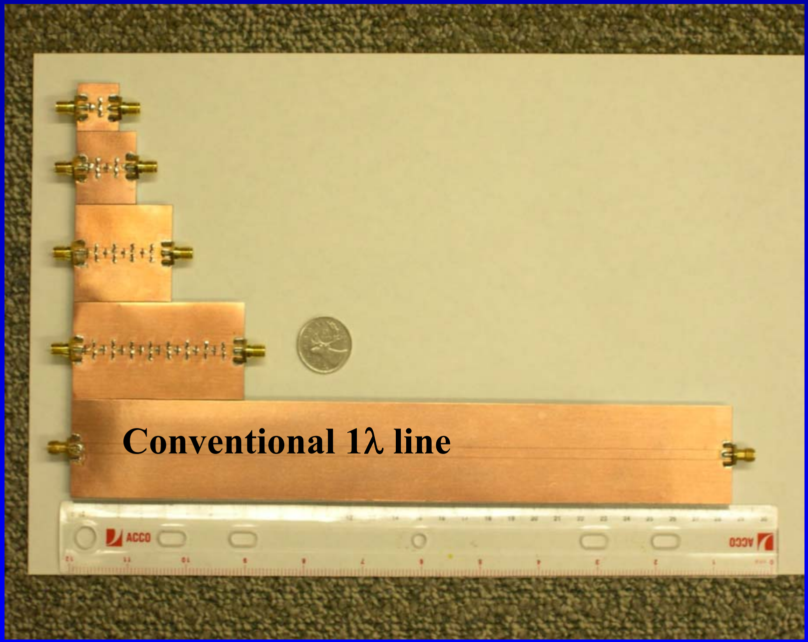

Measured vs. Simulated

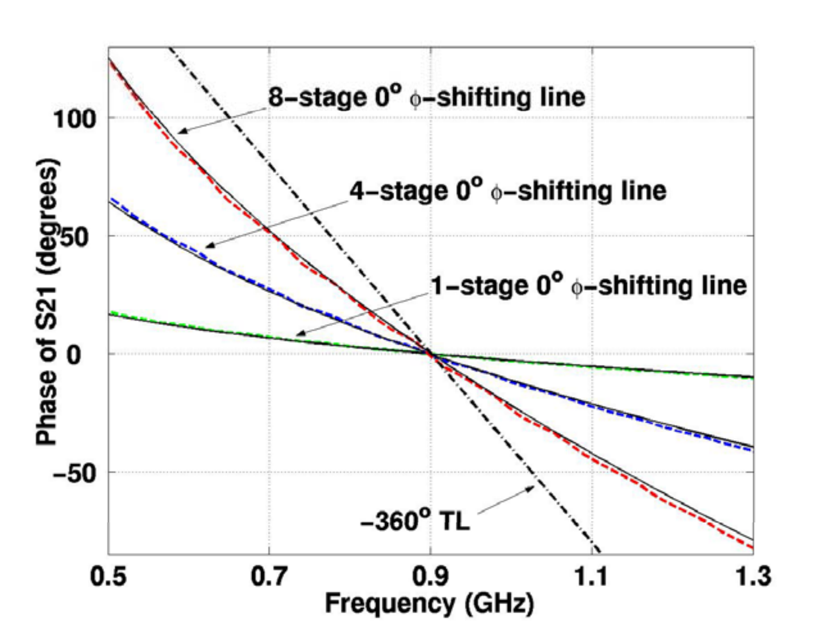

M. Antoniades and G.V. Eleftheriades, "Compact, Linear, Lead/Lag Metamaterial Phase Shifters for Broadband Applications," *IEEE Antennas and Wireless Propagation Letters*, vol. 2, issue 7, pp. 103-106, July 2003.

COMPACT AND BROADBAND SERIES POWER DIVIDERS

Metamaterial 1:4 Divider

Transmission-Line 1:4 Divider

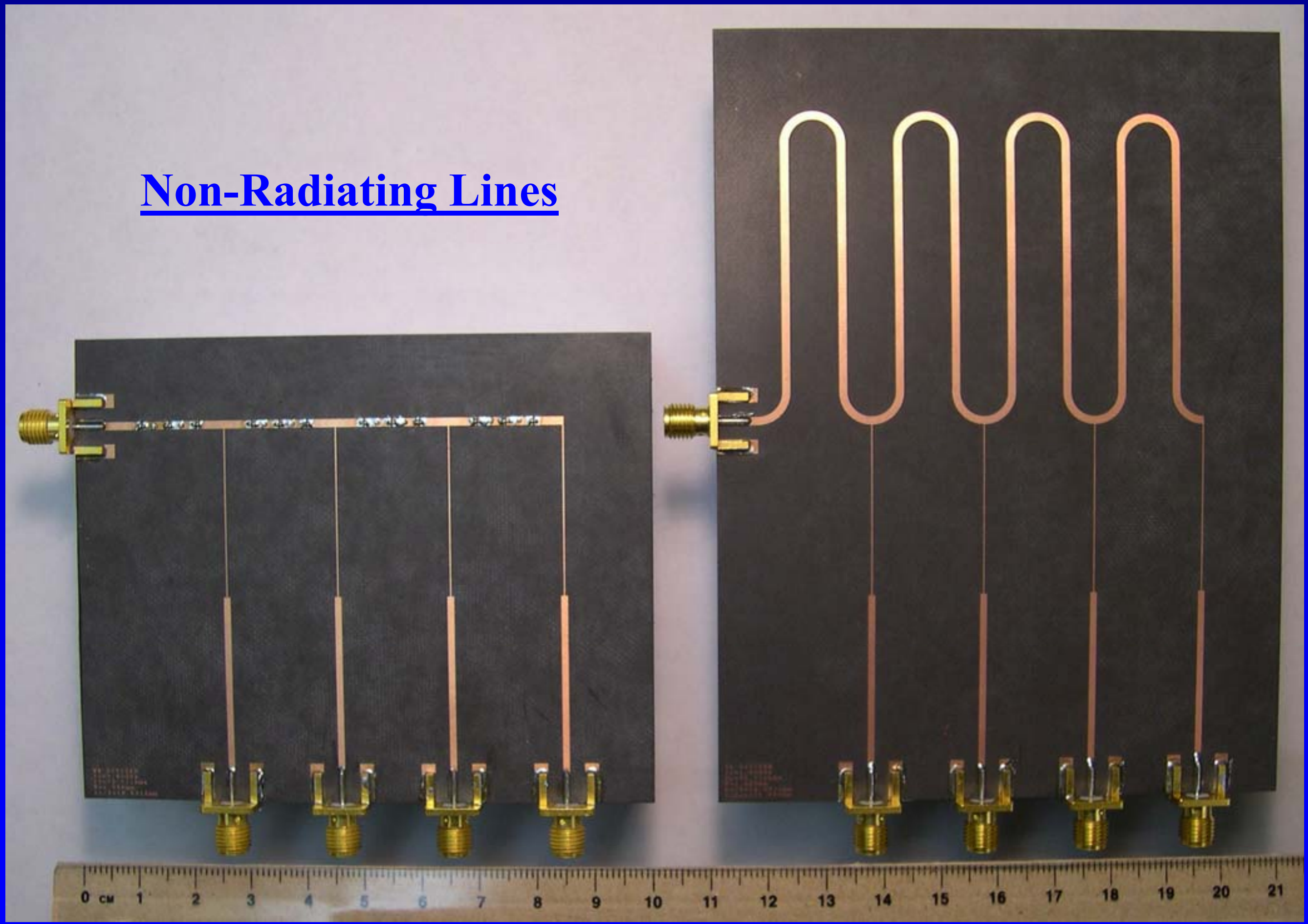

DRAMATIC AREA REDUCTION

BROADBAND:

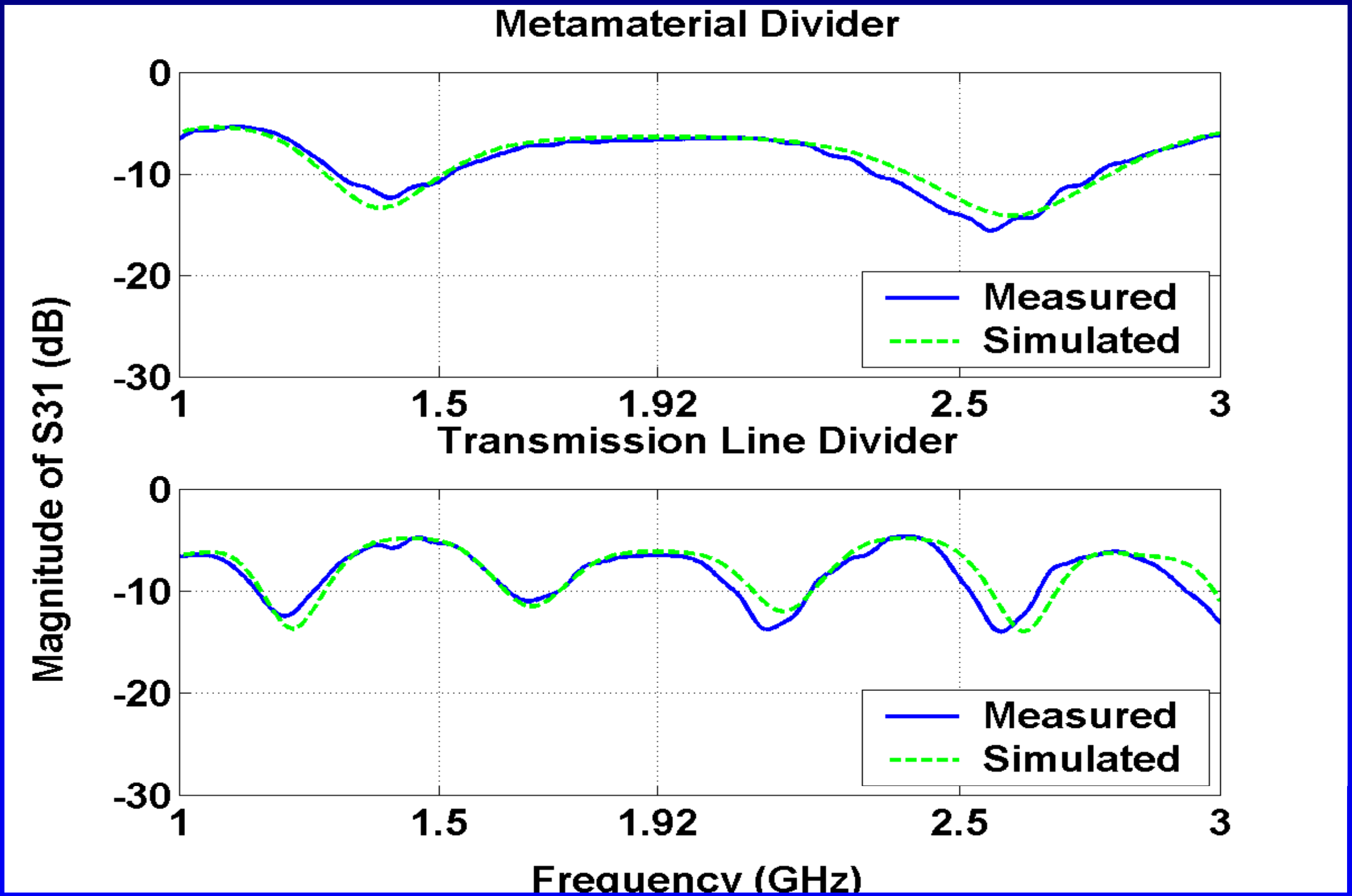

M. Antoniades and G.V. Eleftheriades, "A Broadband Series Power Divider Using Zero-Degree Metamaterial Phase-Shifting Lines", *IEEE MWCL*, Nov. 2005

Tunable MMIC NRI-TL Phase Shifter

0.13μm CMOS MMIC zero-degree phase-shifter (active inductors)

(RH-TLs replaced by lumped L-C sections to reduce size → Integration)

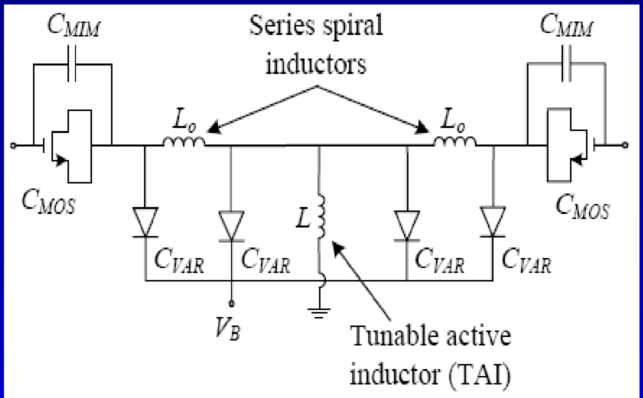

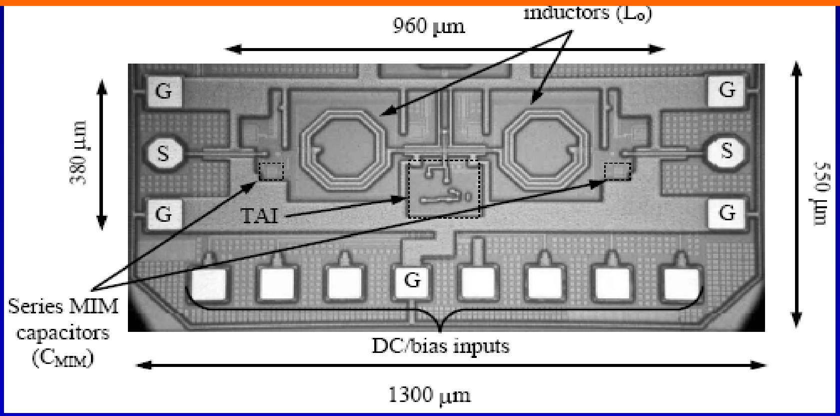

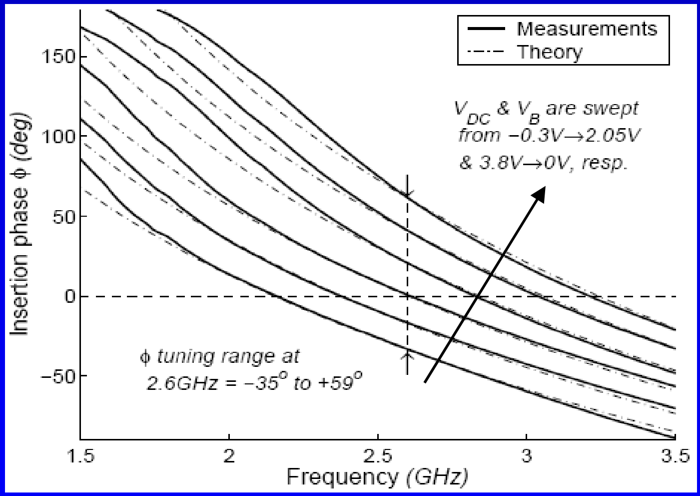

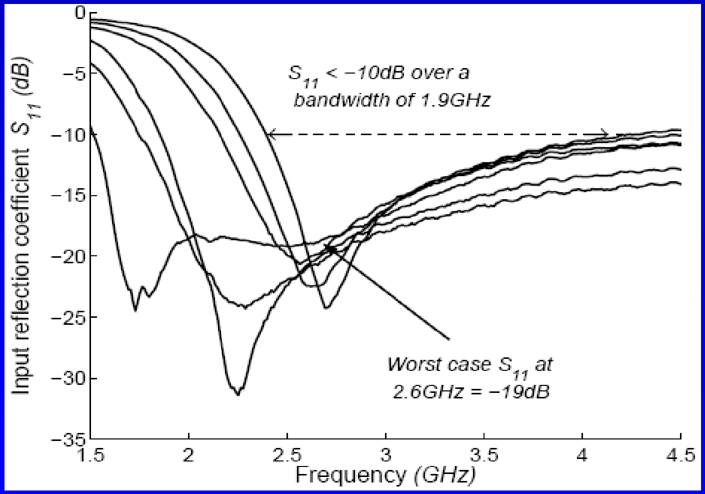

The phase ϕ of a unit-cell can be electronically tuned from -35° to +59° at 2.6GHz, while maintaining S_{11}<-19dB. Across the entire phase tuning range S_{21} varies from -2.8dB to -3.8dB at 2.6GHz.

M.A.Y. Abdalla, K. Phang and G.V. Eleftheriades, "Printed and integrated CMOS positive/negative refractive-index phase shifters using tunable active inductors," *IEEE Trans. Microw. Theory Tech.*, vol. 8, August 2007.

Steerable Series-fed Patch Array

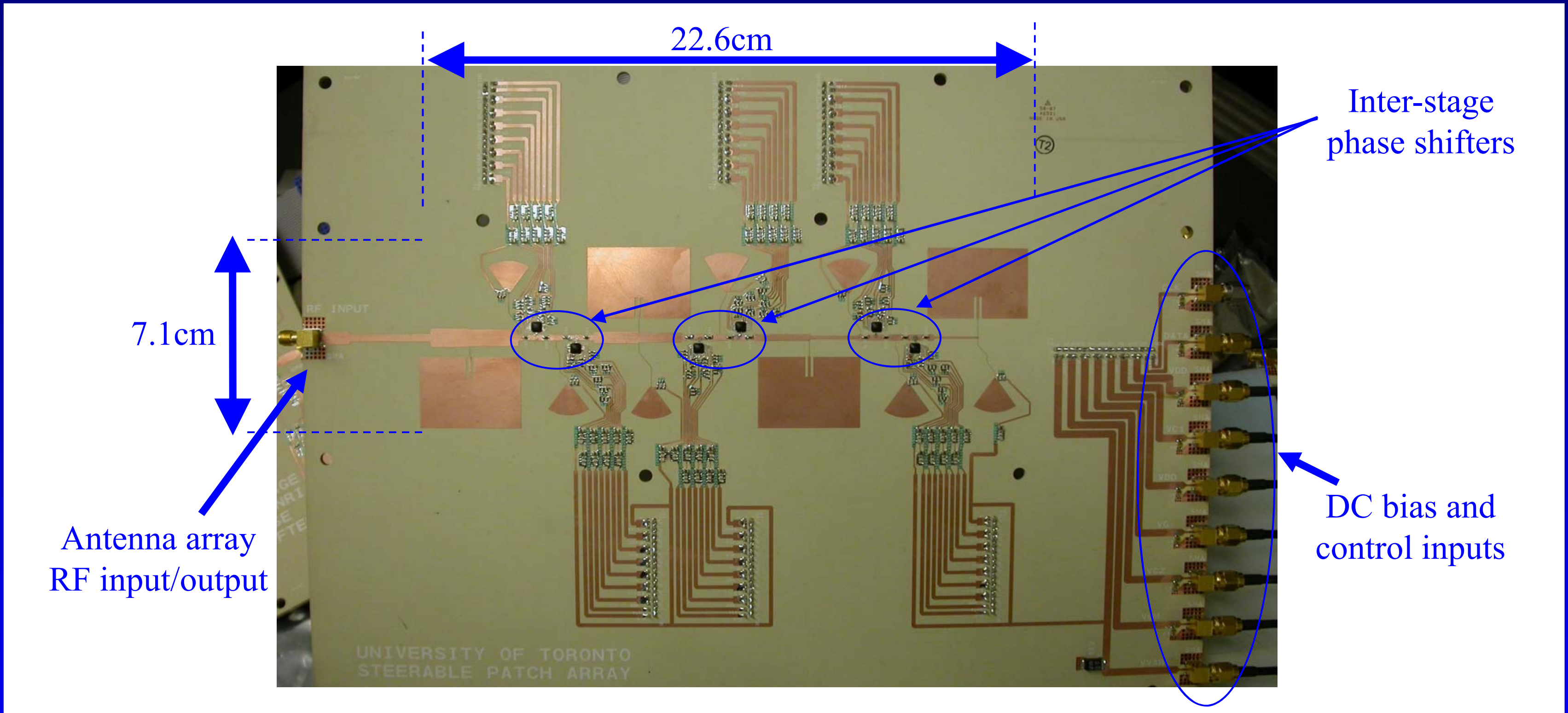

- The array consists of 4 patch antennas and uses 3 inter-stage phase shifters
- The entire antenna array (which includes: patches, feed-lines, and the phase shifters) is designed on a single 2-layer board
- All the inter-stage phase shifter receive the bias and control signals from a ribbon cable on the bottom side of the board

M.A.Y. Abdalla, K. Phang, and G.V. Eleftheriades, "A steerable series-fed phased array architecture using tunable PRI/NRI phase shifters", Intl. Workshop on Antenna Technology (IWAT), March 4-6, Chiba University, Japan, March 4-6, 2008.

Experimental Results

The measured gain patterns versus the azimuthal angle

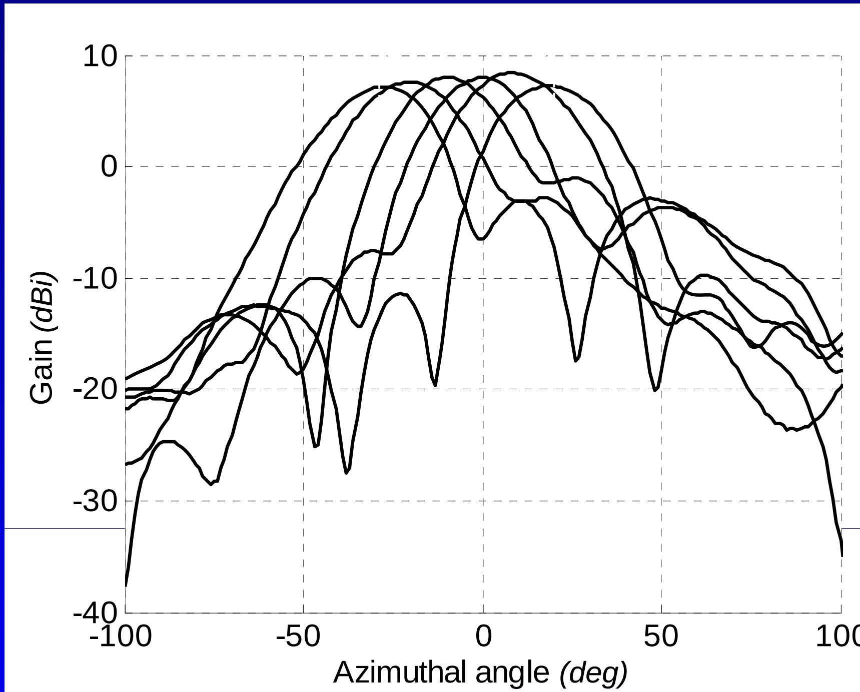

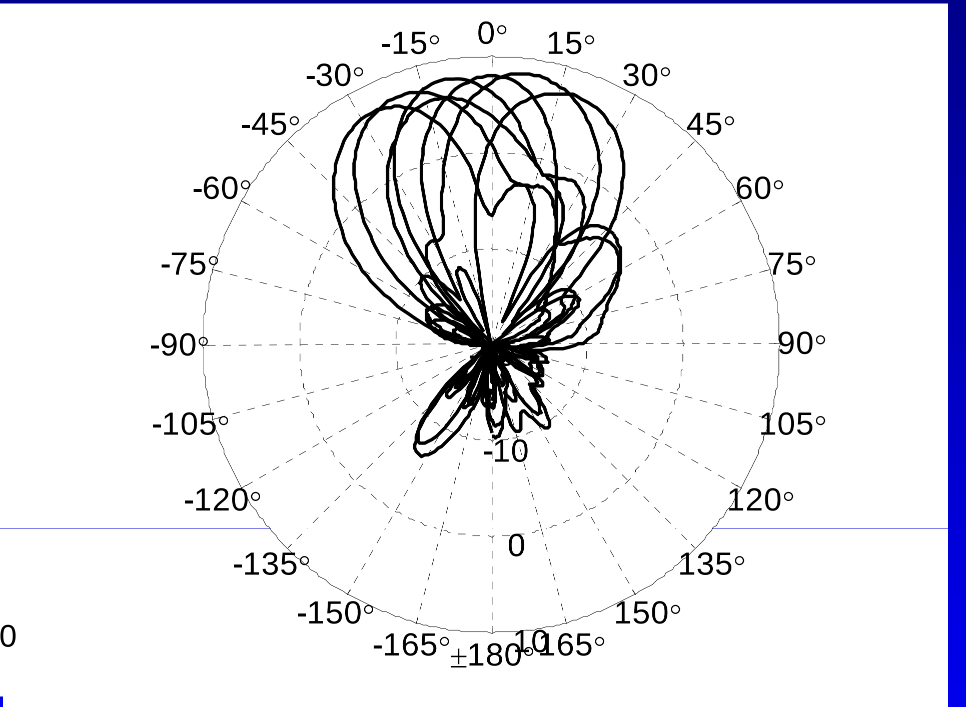

- The measured scan angle ranges from +18° to -27° at 2.4GHz by changing the TAI bias voltages and the varactor control voltage from 3V to 15V.
- The antenna gain changes from 8.4 to 7.1dBi across the entire 45° scan angle range
- Relative side-lobe level < -10dB
- Very little beam-squinting vs frequency

M. A.Y. Abdalla, K. Phang, and G.V. Eleftheriades "A planar electronically steerable patch array using tunable PRI/NRI phase shifters," *IEEE Trans. on Microwave Theory and Techniques,* vol. 57, pp. 531-541, March 2009.

Electrically Small NRI-TL Zero-Index Antennas

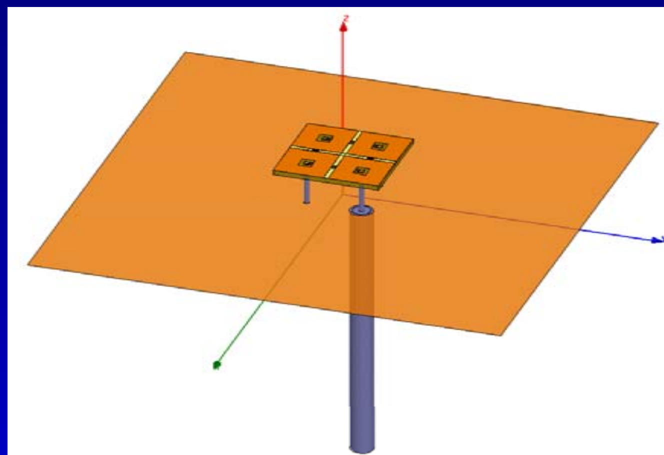

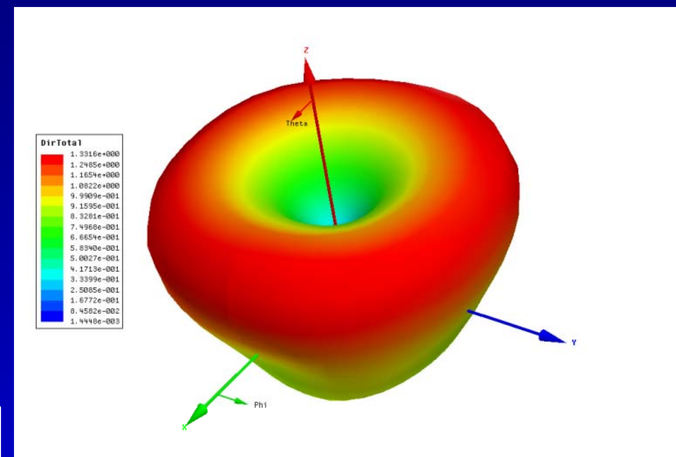

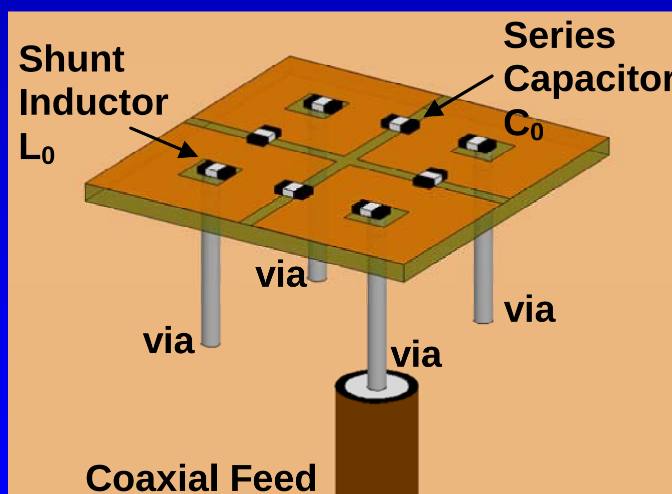

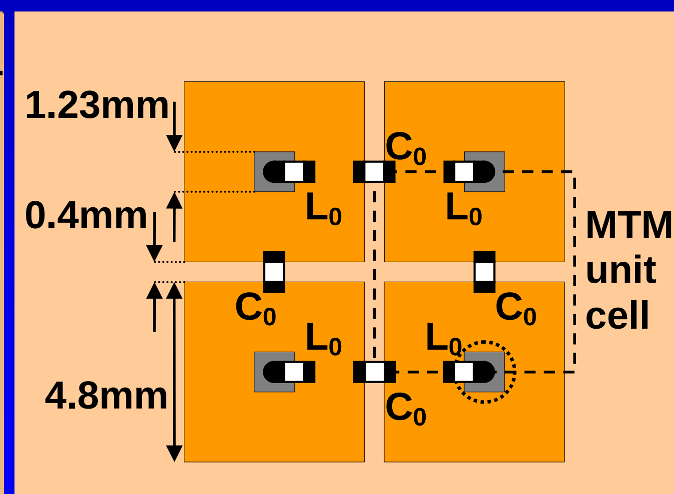

Main idea: Wrap around a 0° MTM phase-shifting line to make a small resonant antenna

G.V. Eleftheriades, A. Grbic, M. Antoniades, "Negative-Refractive-Index Transmission-Line Metamaterials and Enabling Electromagnetic Applications," 2004 *IEEE Antennas and Propagation Society International Symposium Digest*, pp. 1399-1402, Monterey, CA, USA, June 20-25, 2004.

Measured Antenna Patterns

Measured radiation efficiency up to 70-80%
Bandwidth: 1-3% (-10dB point)

W x L x H = $\lambda_0/11$ x $\lambda_0/14$ x $\lambda_0/31$

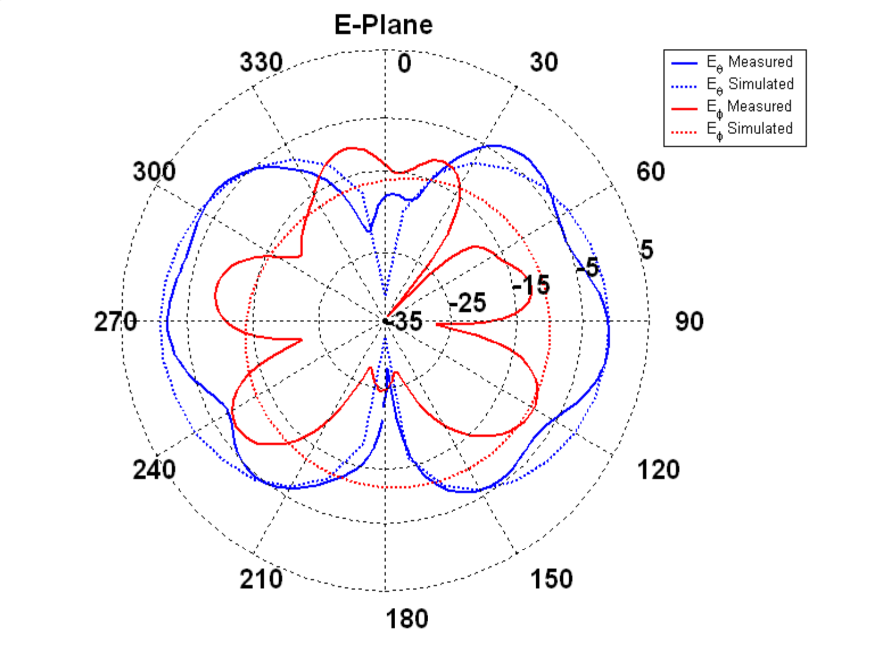

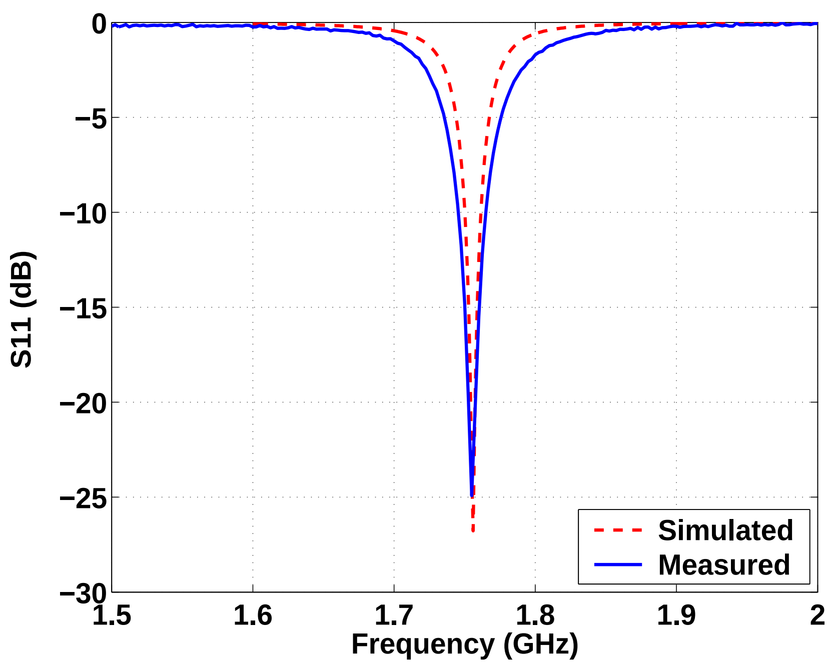

M.A. Antoniades and G.V. Eleftheriades, “A folded-monopole model for electrically small NRI-TL metamaterial antennas," *IEEE Antennas and Wireless Propagat. Letters,* vol. 7, pp. 425-428, 2008.

A Compact Zero-Index NRI-TL Metamaterial Antenna with Extended Bandwidth (double-tuned matching)

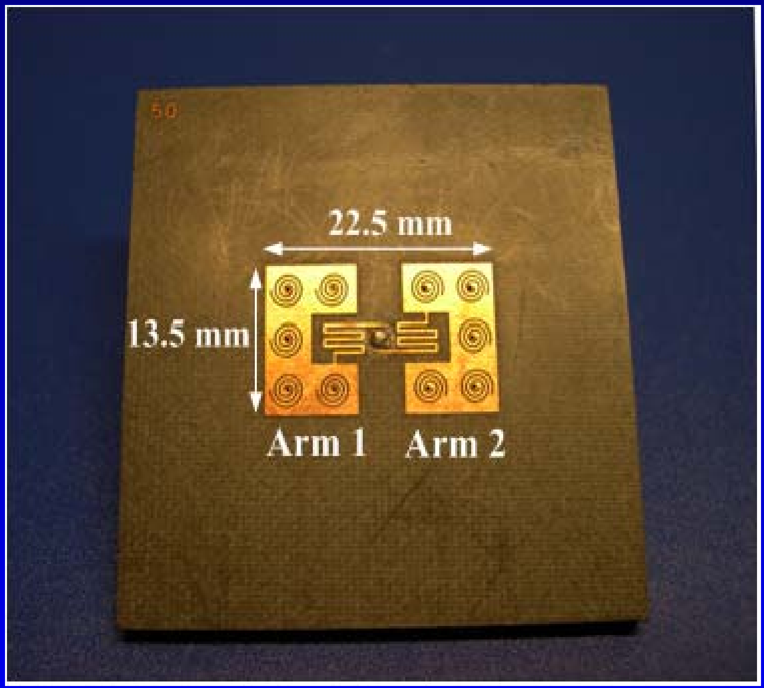

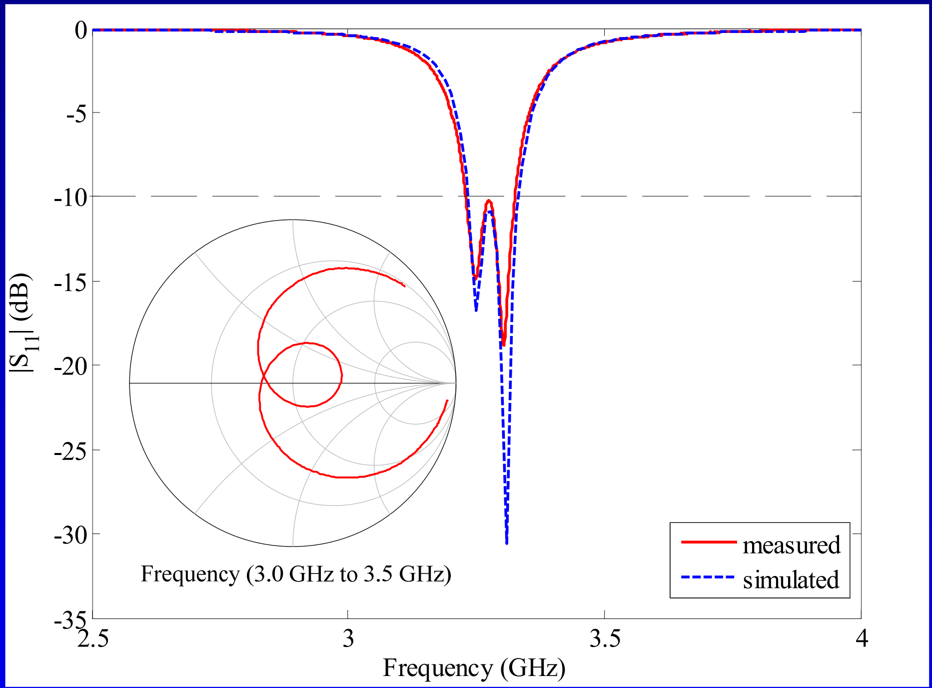

1. Doubly resonant MTM Structure

2. More than doubled the bandwidth compared with the singly resonant MTM antenna

J. Zhu and G.V. Eleftheriades, "A compact transmission-line metamaterial antenna with extended bandwidth," *IEEE Antennas and Wireless Propagat. Letters , vol. 08, pp. 295-298, 2009.*

'DUAL-MODE' BROADBAND NRI-TL MONOPOLE

Unloaded monopole antenna

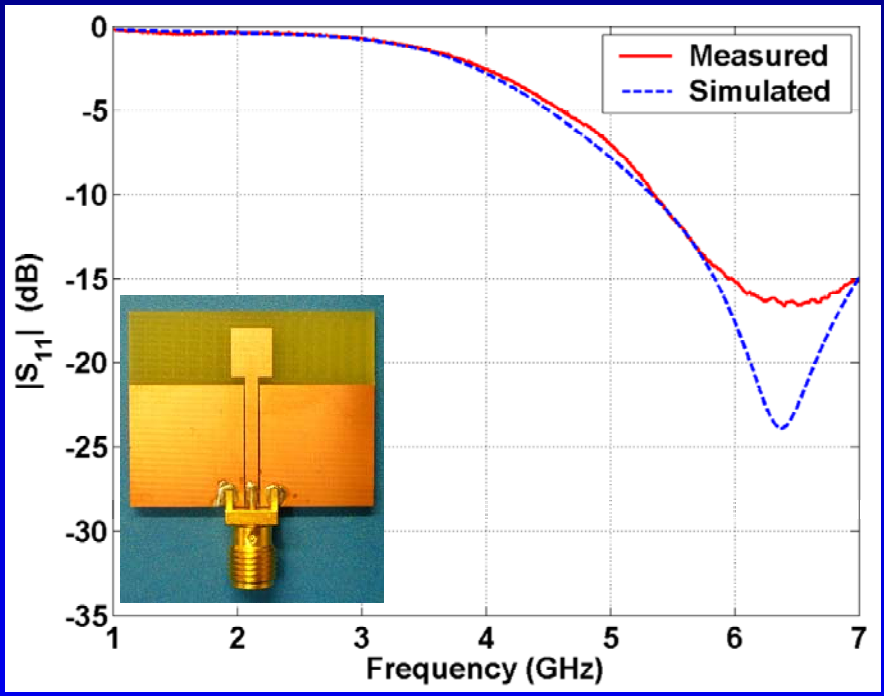

Single NRI-TL cell loaded monopole

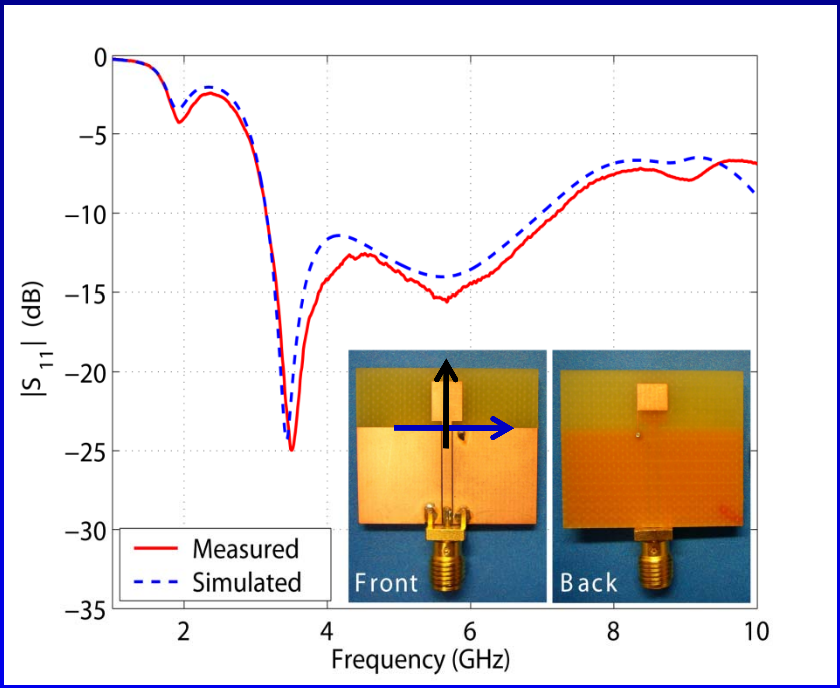

A single resonance at 6.4 GHz

A dual resonance at 3.5 GHz and 5.5 GHz.

BW_{-10dB} = 3.78GHz

M.A. Antoniades and G.V. Eleftheriades, "A broadband dual-mode monopole antenna using NRI-TL metamaterial loading," *IEEE Antennas and Wireless Propagat. Letters.*, vol 8, pp. 258-261, 2009.

High-Directivity Coupled-Line Coupler

Coupled Microstrip/NRI TLines:

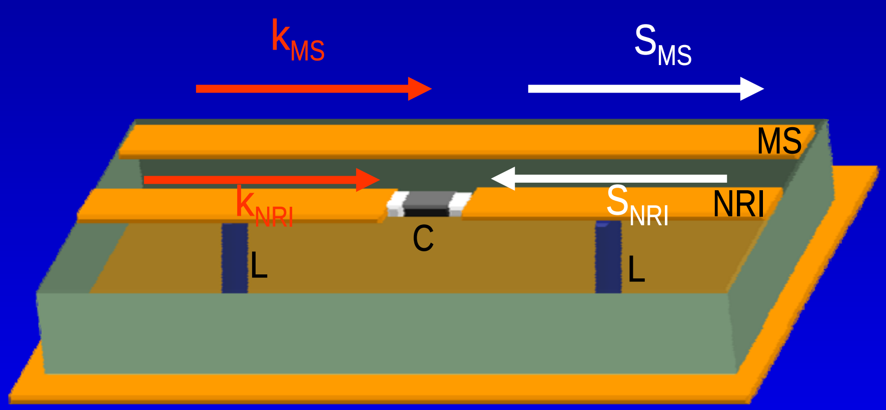

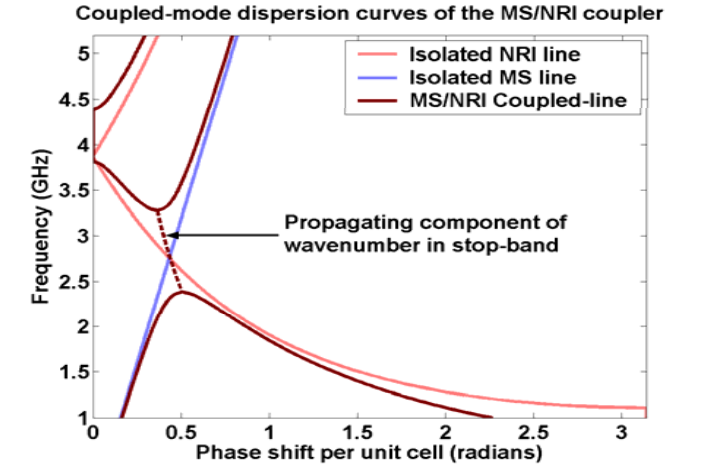

Co-directional phase flow but contra-directional power flow!

R. Islam and G.V. Eleftheriades, "A planar metamaterial co-directional coupler that couples power backwards." 2003 IEEE Itnl. Microwave Symposium Digest, Philadelphia, June 8-13, pp. 321-324, 2003.

Conventional Microstrip vs. MS/NRI Coupled-Line Coupler

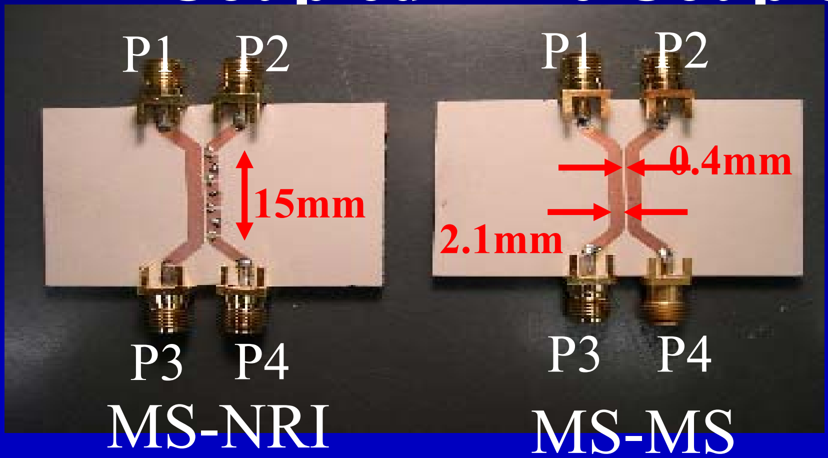

- Equal length
- Equal line spacing
- Equal propagation constant

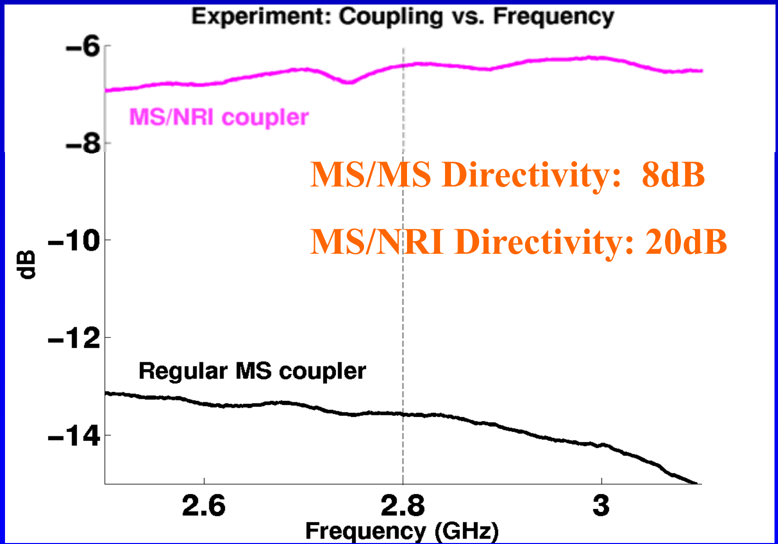

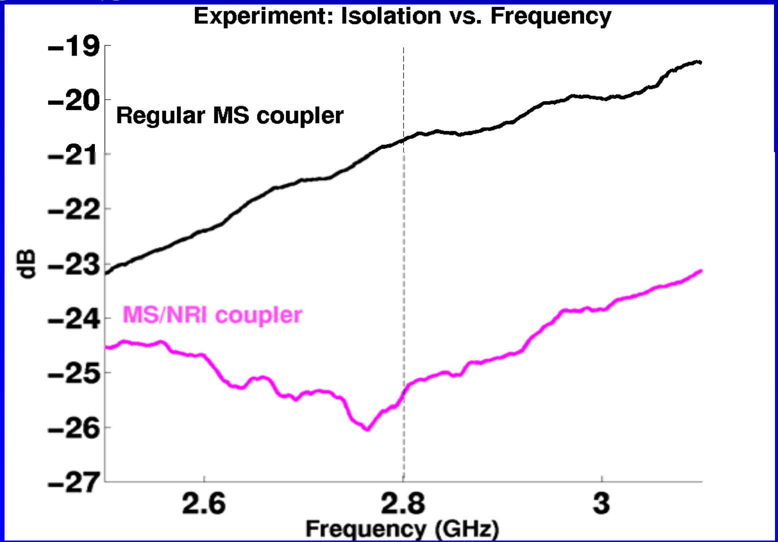

R. Islam and G.V. Eleftheriades, "A planar metamaterial co-directional coupler that couples power backwards." 2003 IEEE Itnl. Microwave Symposium Digest, Philadelphia, June 8-13, pp. 321-324, 2003.

Metamaterial MS/NRI 3dB Coupler

- Operates in coupled mode stop band
- Arbitrary coupling levels by increasing coupler length

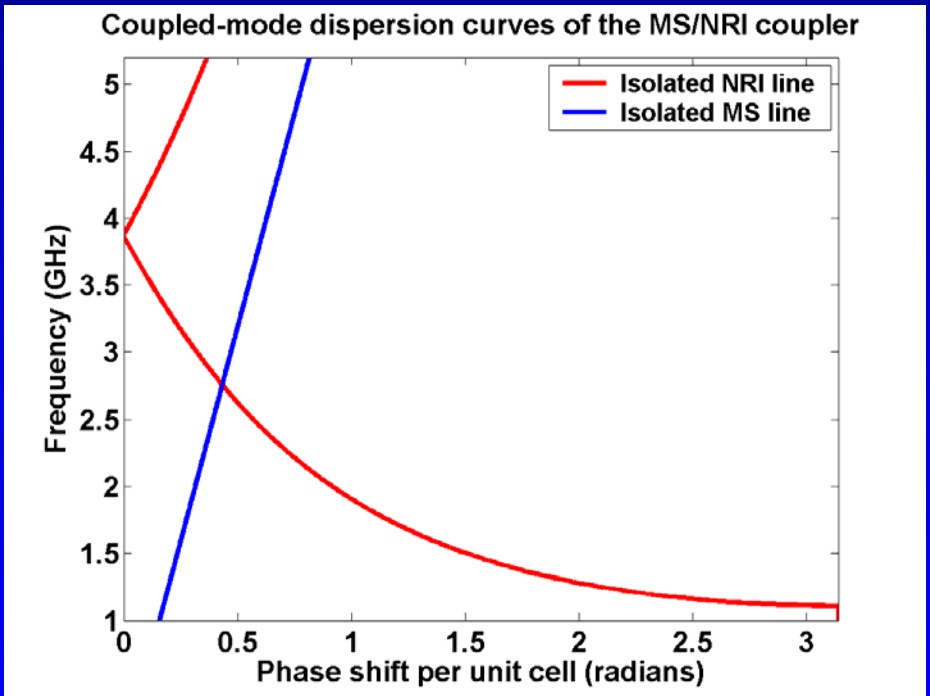

Metamaterial MS/NRI 3dB Coupler

- Operates in coupled mode stop band
- Arbitrary coupling levels by increasing coupler length

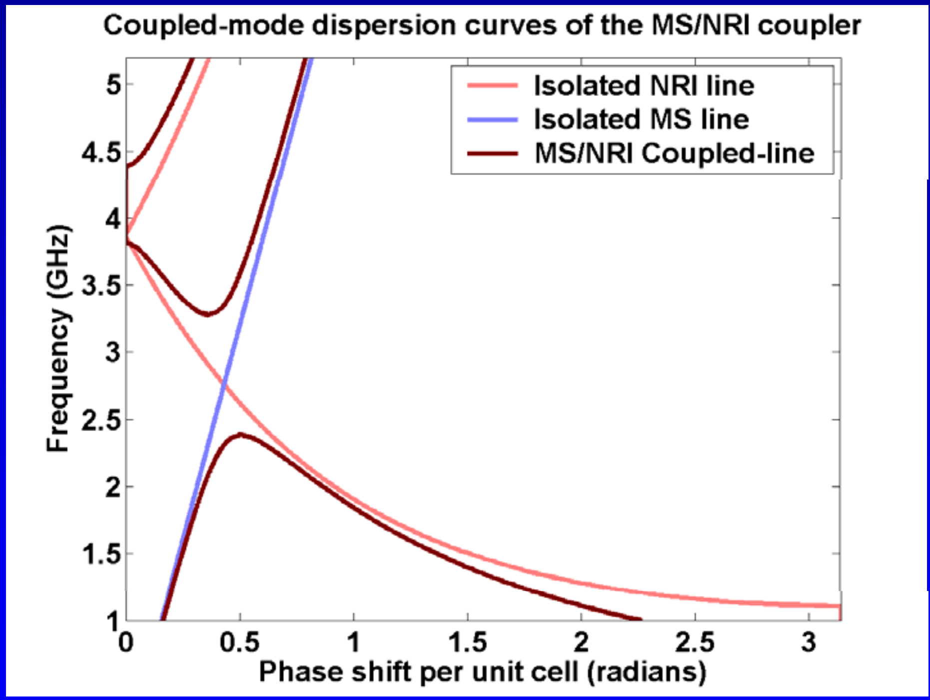

Metamaterial MS/NRI 3dB Coupler

- Operates in coupled mode stop band
- Arbitrary coupling levels by increasing coupler length

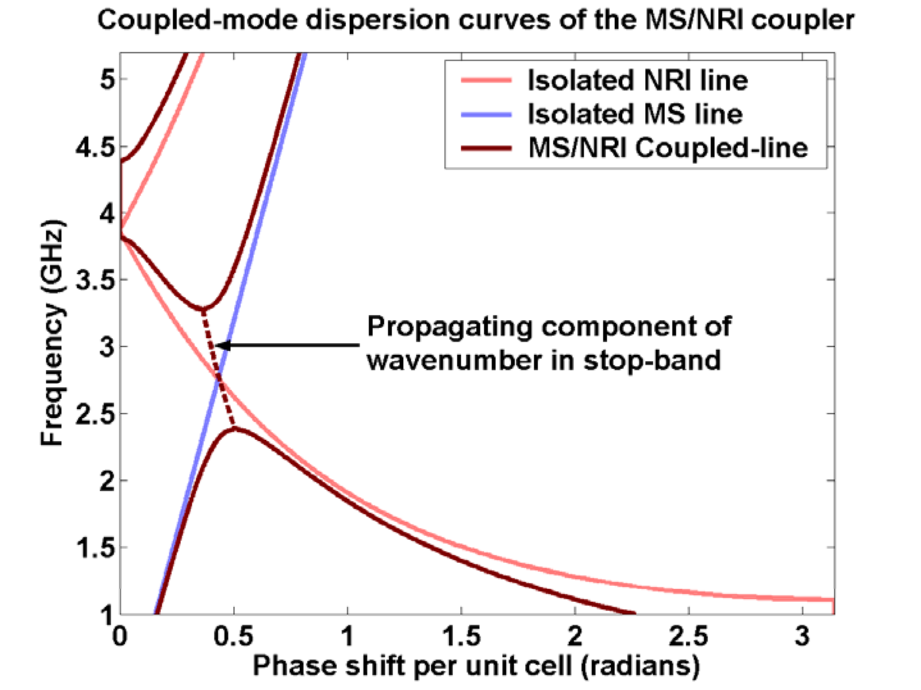

Phase Progression With Exponential Field Variation

R. Islam, F. Elek and G.V. Eleftheriades, "A coupled-line metamaterial coupler having co- directional phase but contra-directional power flow." ***Electronics Letters,*** **vol. 40, no. 5, March 04, 2004.**

Operation in Coupled-Mode Stop Band

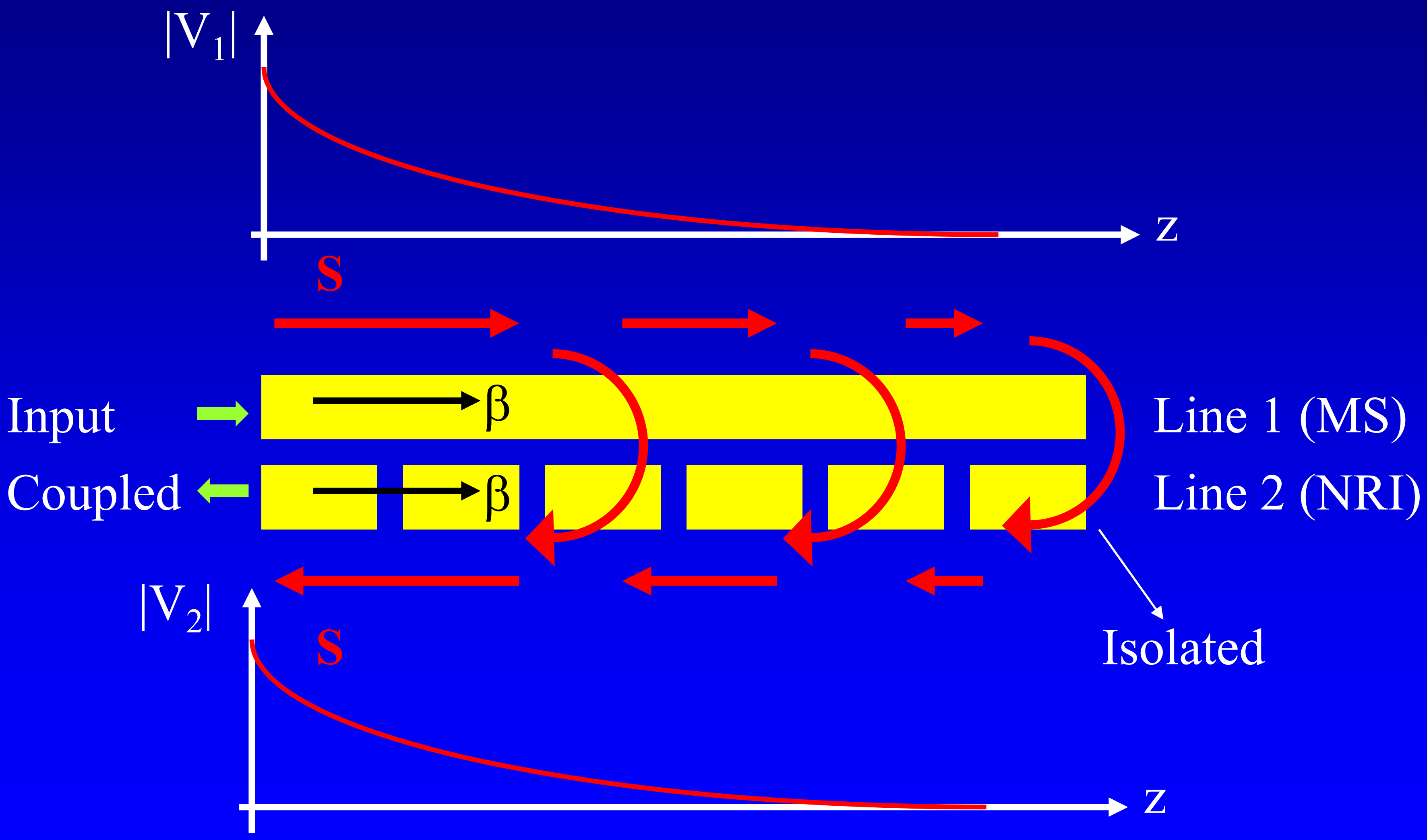

3dB Coupler: Experimental Results

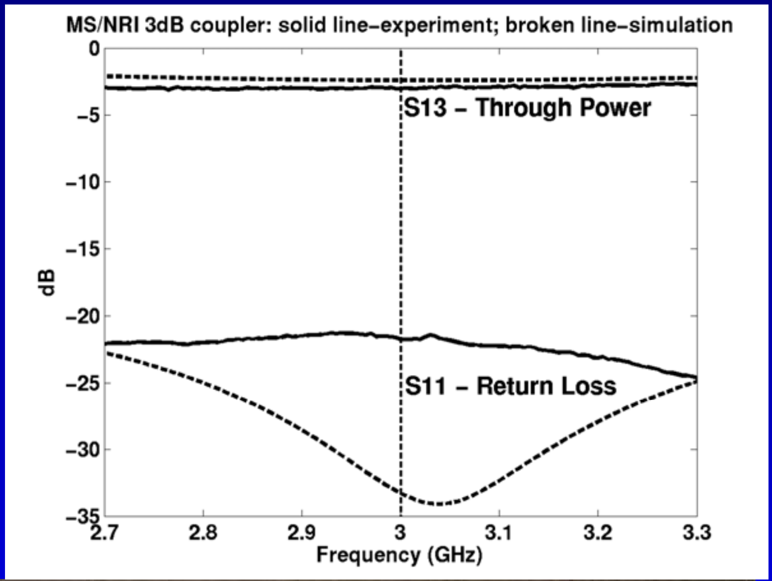

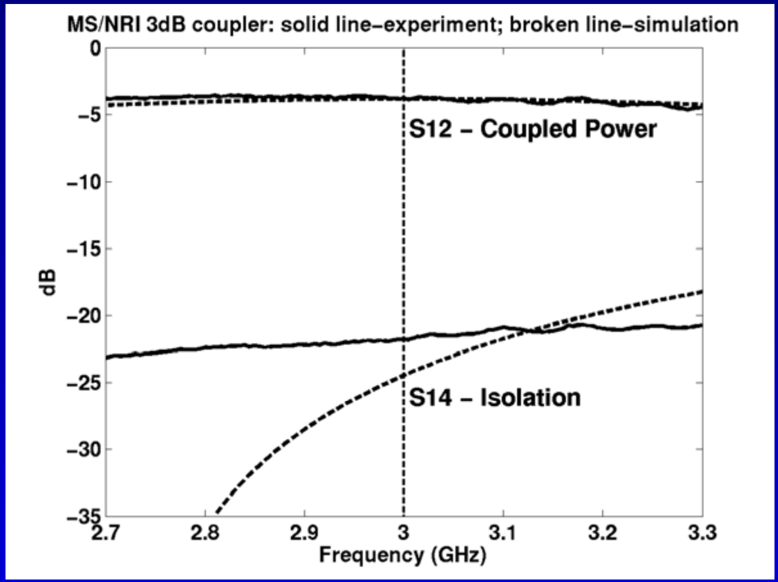

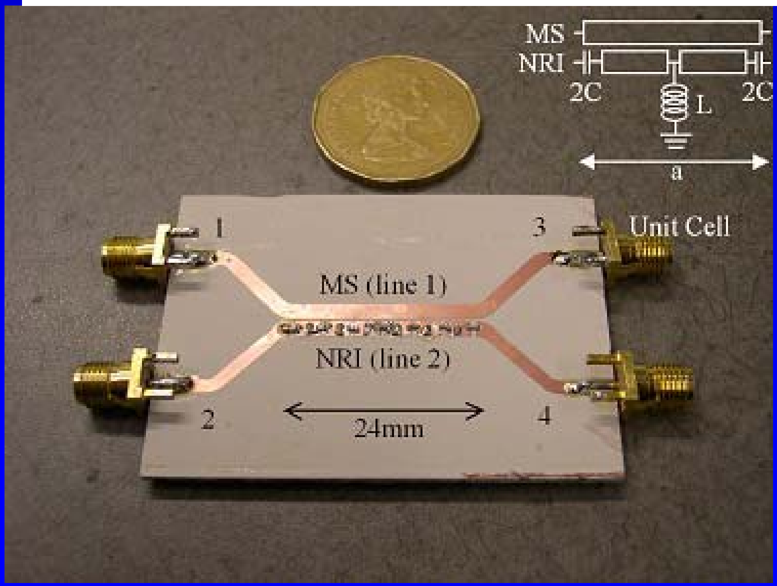

- Operating frequency – 3GHz
- Cell size – 4mm
- Line width – 2.34mm
- C - 1.3pF, L - 3.3nH
- #of unit cells – 6

R. Islam, F. Elek and G.V. Eleftheriades, "A coupled-line metamaterial coupler having co- directional phase but contra-directional power flow." ***Electronics Letters,*** **vol. 40, no. 5, March 04, 2004.**

FULLY PRINTED HIGH-DIRECTIVITY REFLECTOMETER

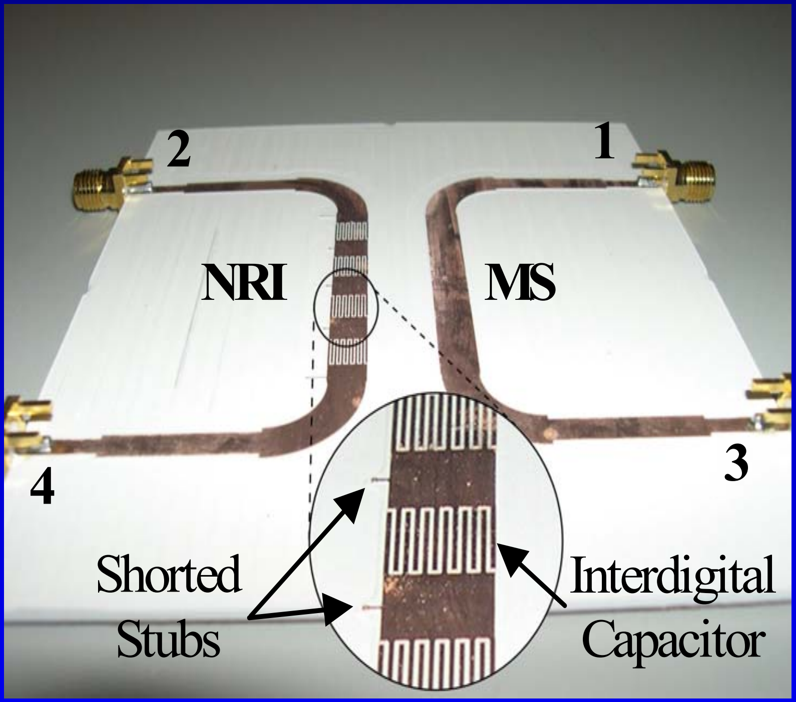

Solid Line: Measured

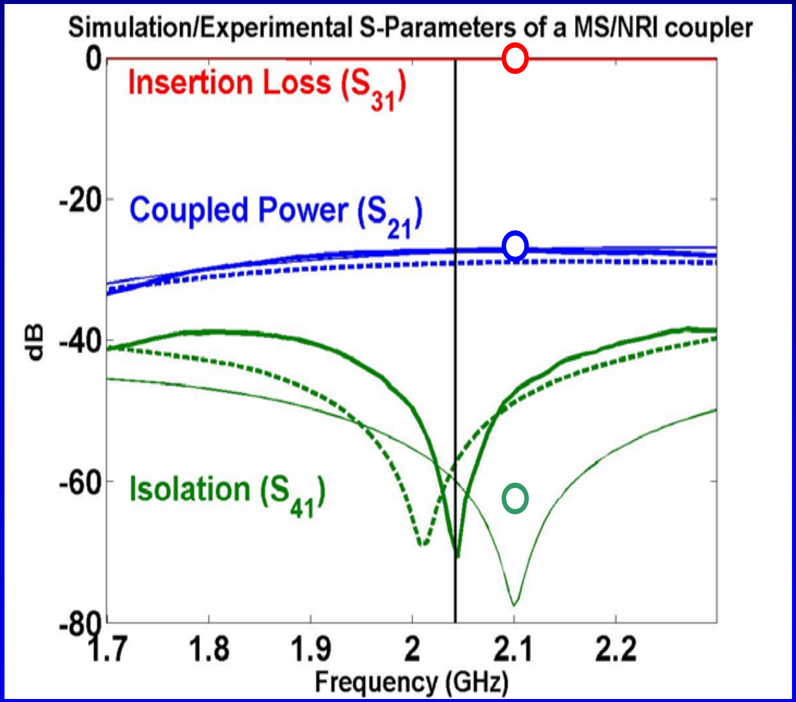

Coupling : –27 dB
Isolation: –72 dB
Directivity: 45 dB

@ f=2.04 GHz

R. Islam and G.V. Eleftheriades, IEEE MWCL, pp. 164-166 April 2006.

2D AND VOLUMETRIC APPLICATIONS: SUPERLENSES

Focusing from Planar n<0 Slabs

Veselago's Lens

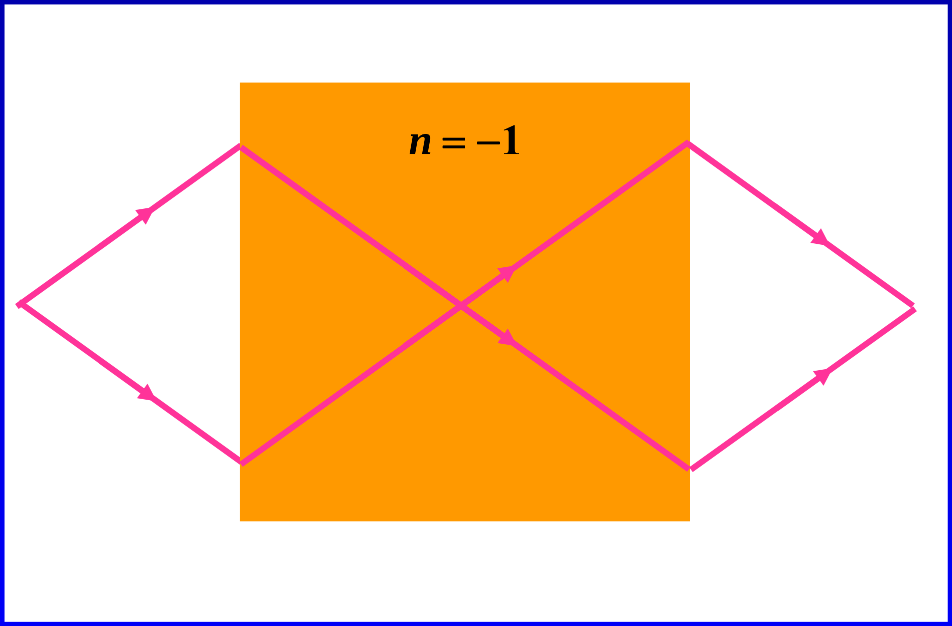

- Flat but homogeneous lens
- Point-to-point focusing
- No optical axis

Negative-Refractive-Index (NRI) Lens

ISOTROPIC 3D NRI-TL METAMATERIAL

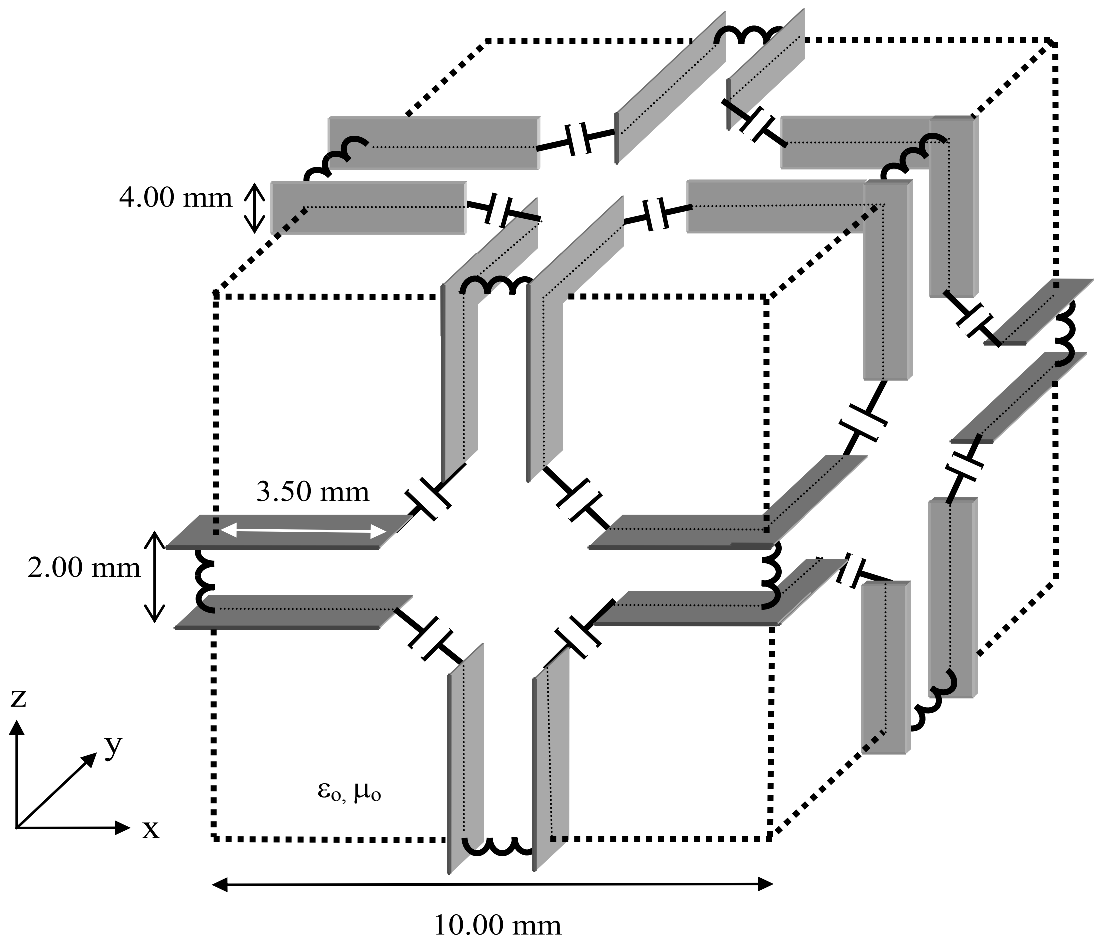

A. Grbic and G.V. Eleftheriades, "An isotropic three-dimensional negative-refractive-index transmission-line metamaterial," ***Journal of Applied Physics,*** **98, pp. 043106, Aug. 15 (2005).**

VOLUMETRIC "STACKED" NRI-TL MEDIUM (layer-by-layer fabrication)

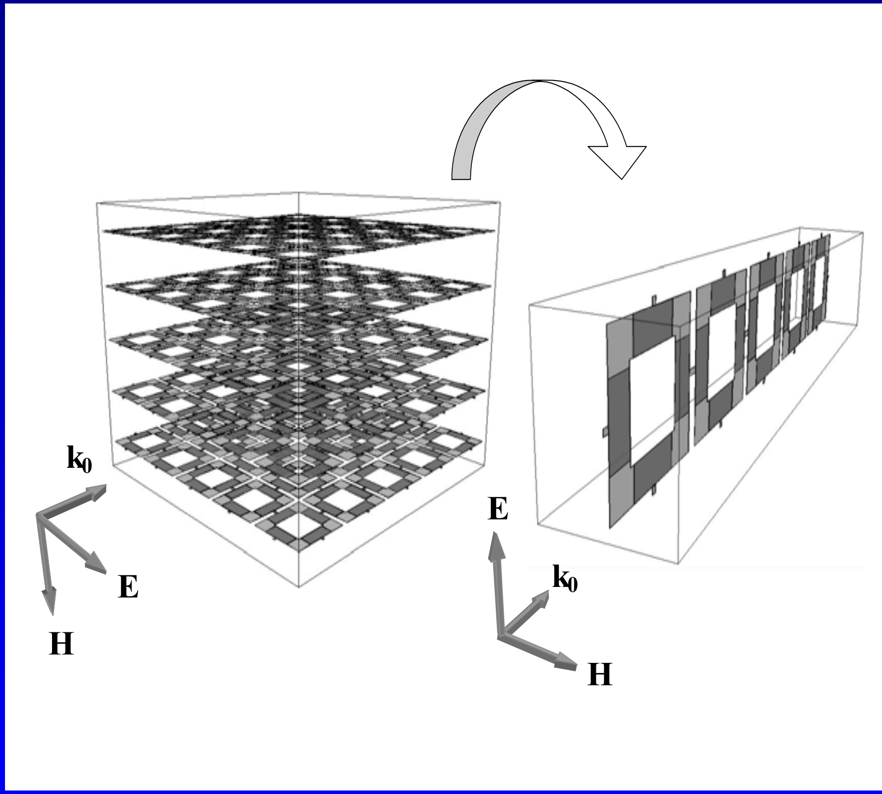

A source embedded in free-space

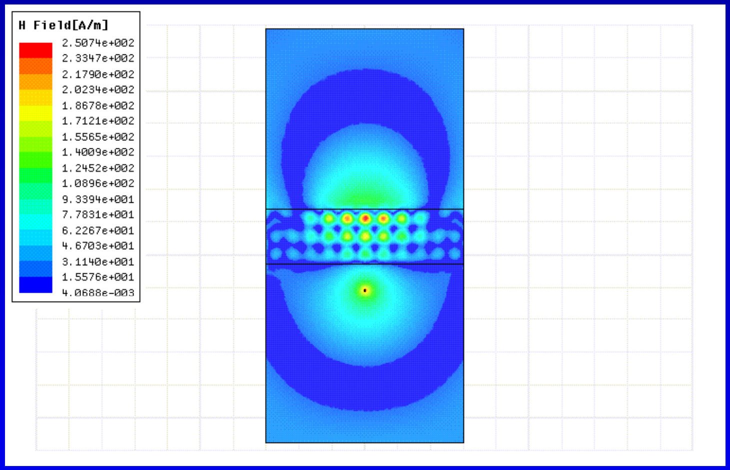

•A.K. Iyer and G.V. Eleftheriades, "A volumetric layered transmission-line metamaterial exhibiting a negative refractive index," *Journal of the Optical Society of America (JOSA-B),* vol. 23, no. 3, pp. 553-570, March 2006.

•A.K. Iyer and G.V. Eleftheriades, "Characterization of a multilayered negative-refractive-index transmission-line (NRI-TL) metamaterial," *IEEE Intl. Microwave Symposium (IMS)*, San Francisco, CA, June 11-16, 2006.

NEGATIVE-REFRACTIVE-INDEX TRANSMISSION-LINE (NRI-TL) SUPERLENS

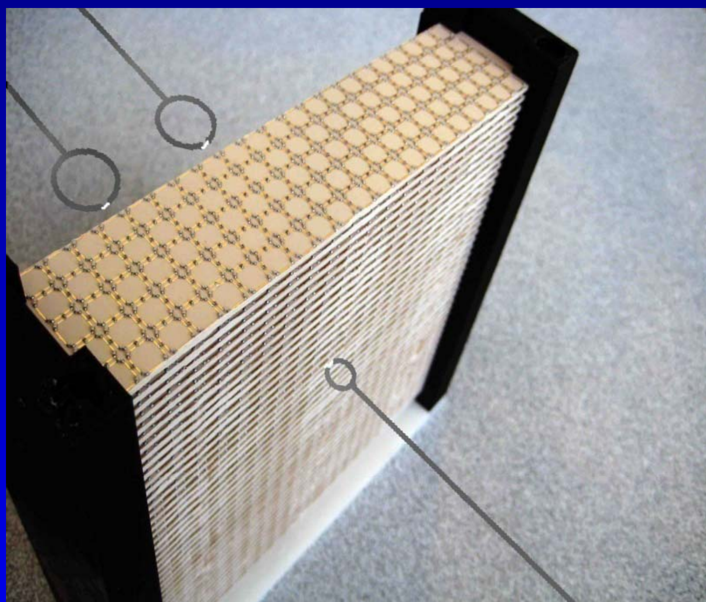

Resolving two sources λ/3 apart @ 2.4GHz
Distance between source and image: 0.57 λ

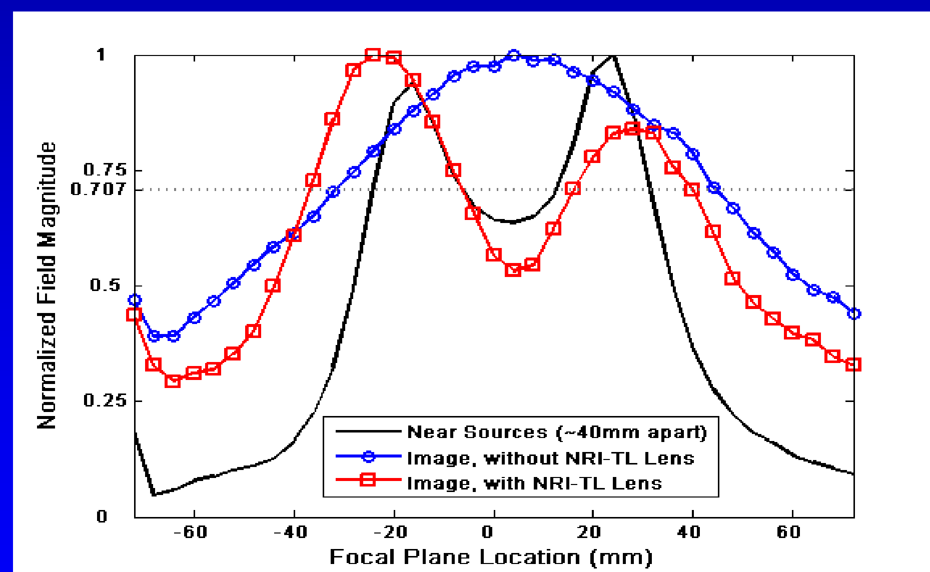

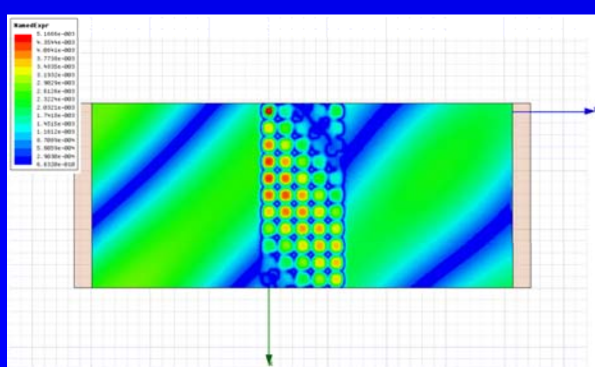

A.K. Iyer and G.V. Eleftheriades, *Appl. Phys. Lett.*, 92, 131105, March 2008.

A.K. Iyer and G.V. Eleftheriades, "Free-space imaging beyond the diffraction limit using a Veselago-Pendry transmission-line metamaterial superlens," *IEEE Trans. Antennas and Propagat.*, vol. 57, pp. 1720-1727, June 2009.

HFSS Simulations

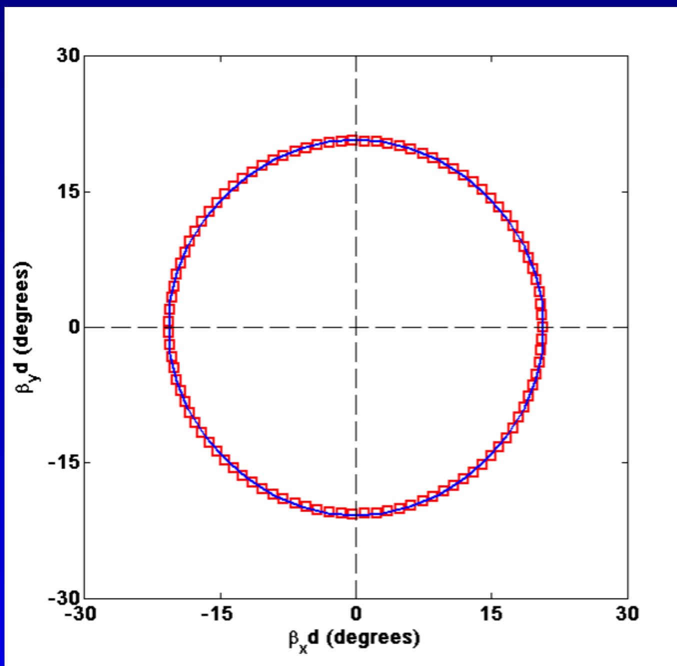

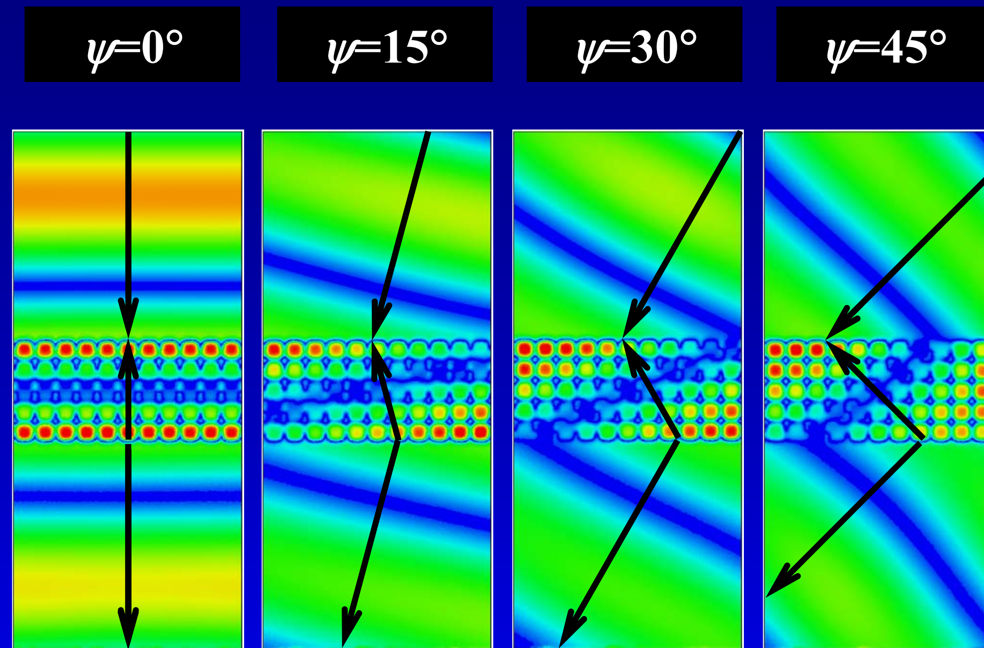

"Isotropic" n = -1 evident from iso-frequency contour at ω_0

Clear Bloch-wavefronts forming (macroscopic)

Transmission-Line MTM Cloaks:

Point Source Adjacent to a Metallic Cylinder

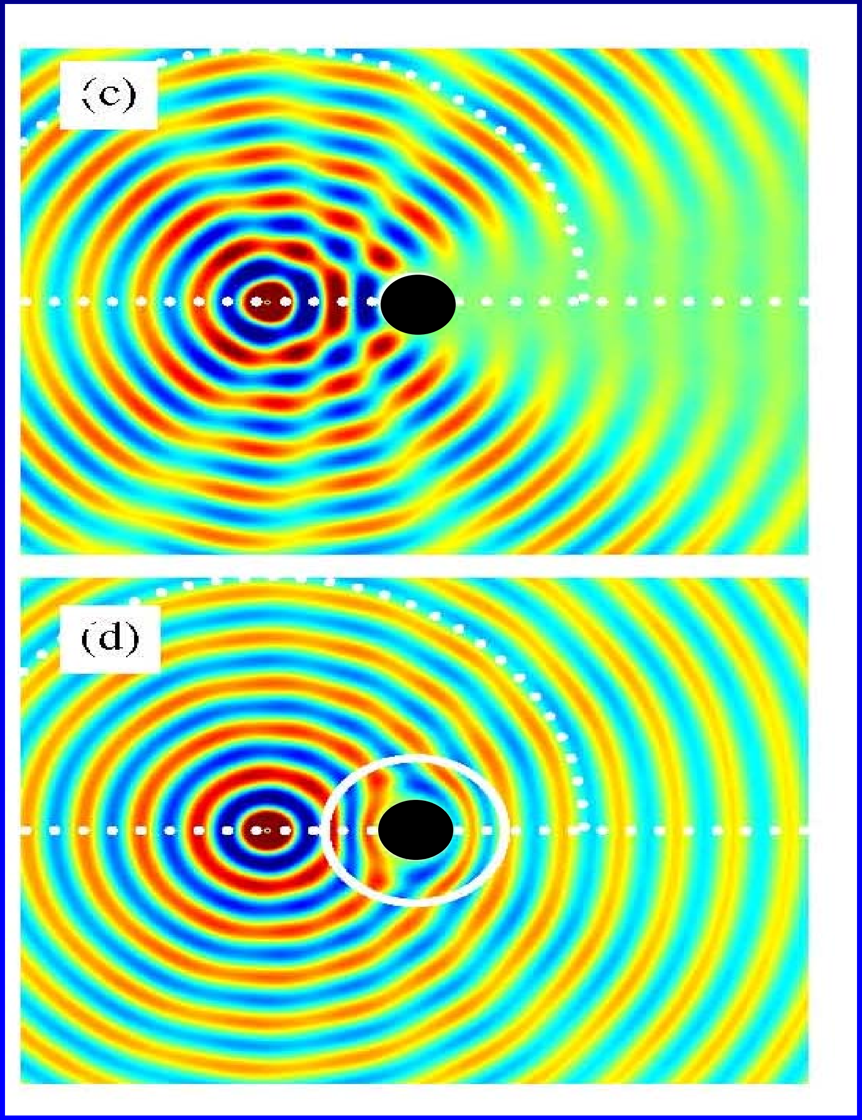

Without TL Cloak

With TL Cloak

M. Zedler and G.V. Eleftheriades, 2009

HYPERBOLIC TL METAMATERIALS

Unit Cell of K.G. Balmain's Anisotropic TL Metamaterial

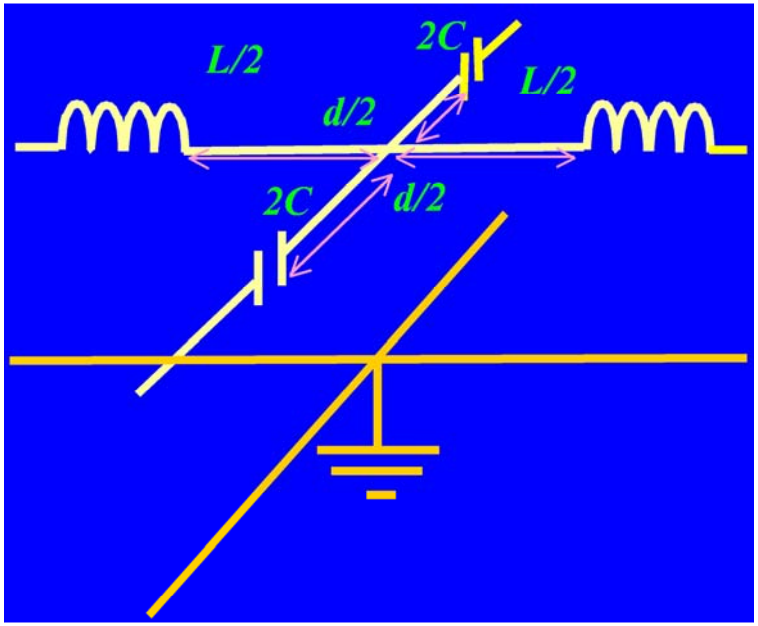

K. G. Balmain, A. A. E. Lüttgen, P. C. Kremer, "Resonance cone formation, reflection, refraction and focusing in a planar anisotropic metamaterial," *IEEE Antennas and Wireless Propagation Letters*, vol. 1, no. 7, pp. 146-149, 2002.

ANISOTROPIC RESONANCE-CONE METAMATERIALS USING CONTINUOUS METALLIC GRIDS OVER GROUND

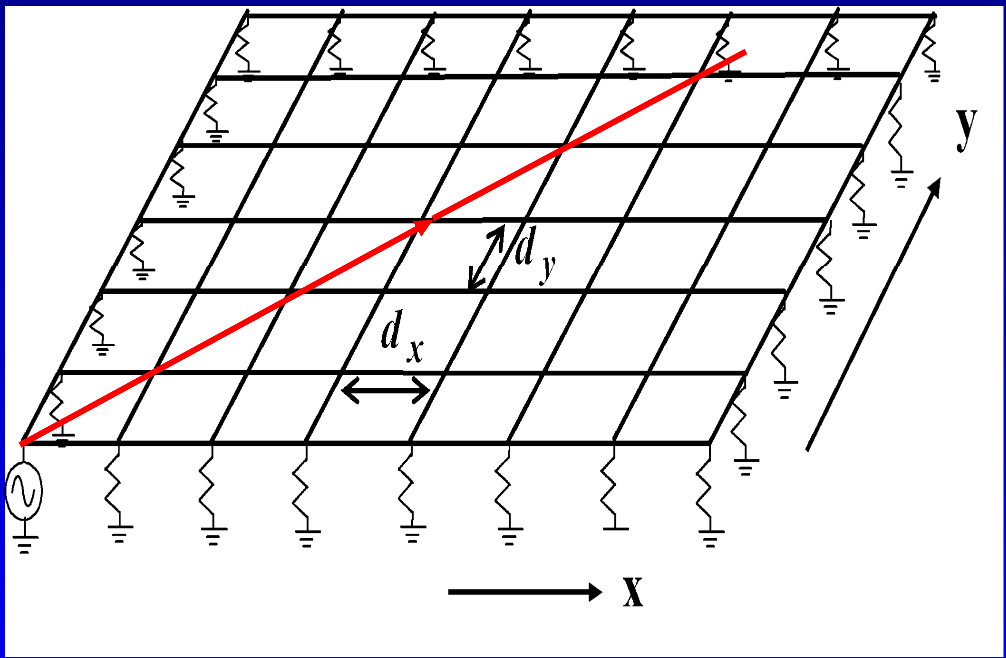

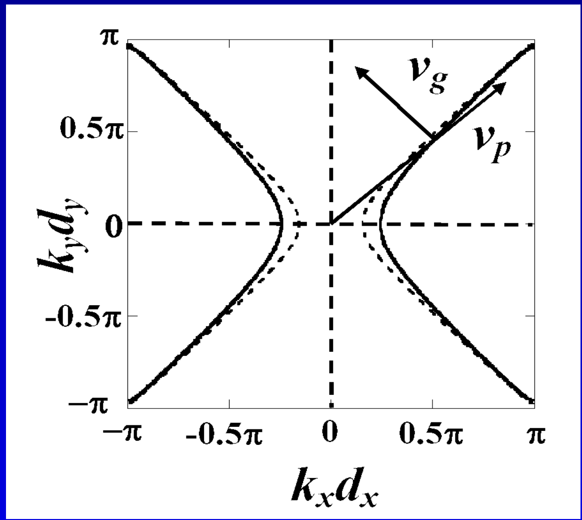

$$\beta_x(f_r)d_x + \beta_y(f_r)d_y = 2\pi$$

NOTE: NO LUMPED ELEMENTS OR VIAS➔SCALABLE

FOCUSING WITH CONTINUOUS HYPERBOLIC GRIDS OVER GROUND

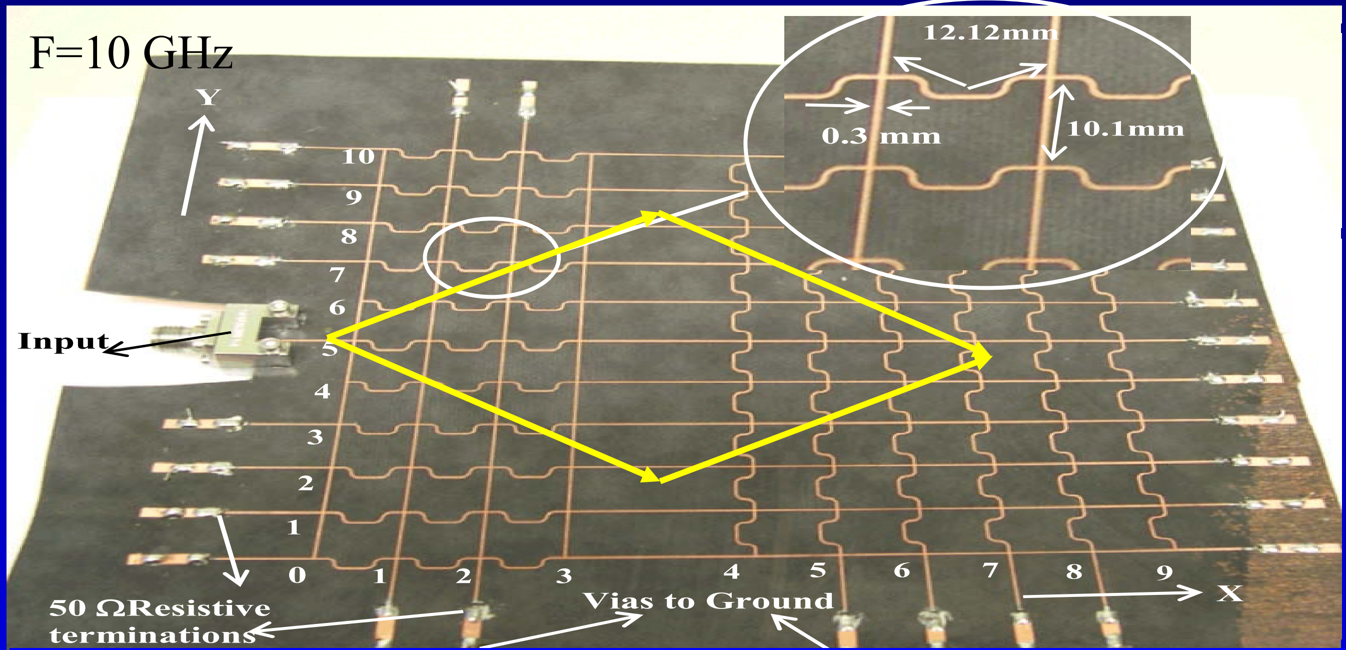

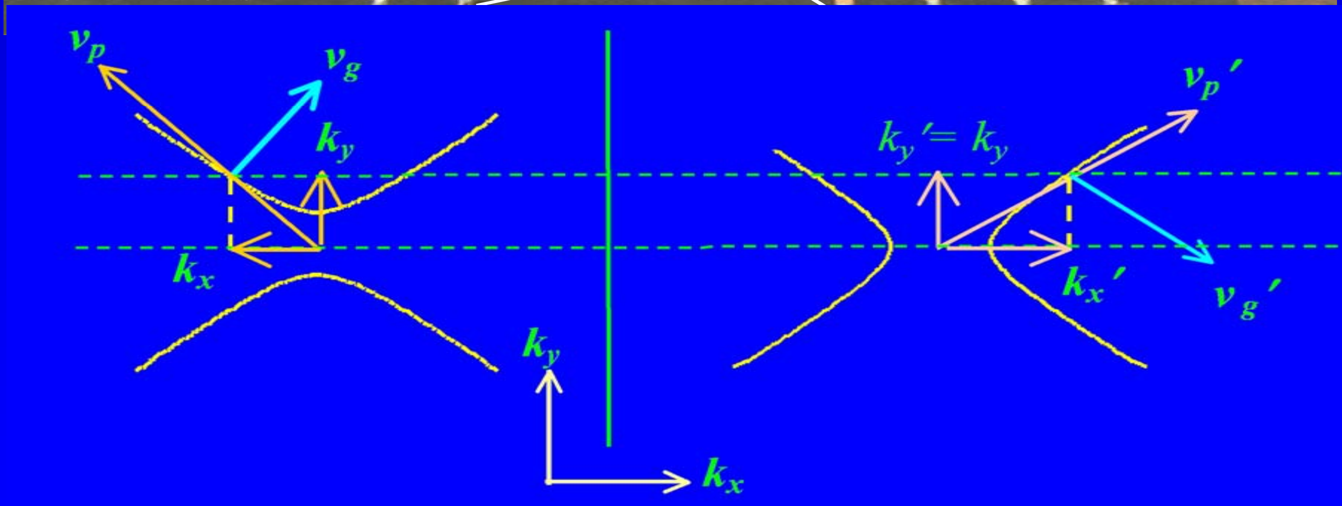

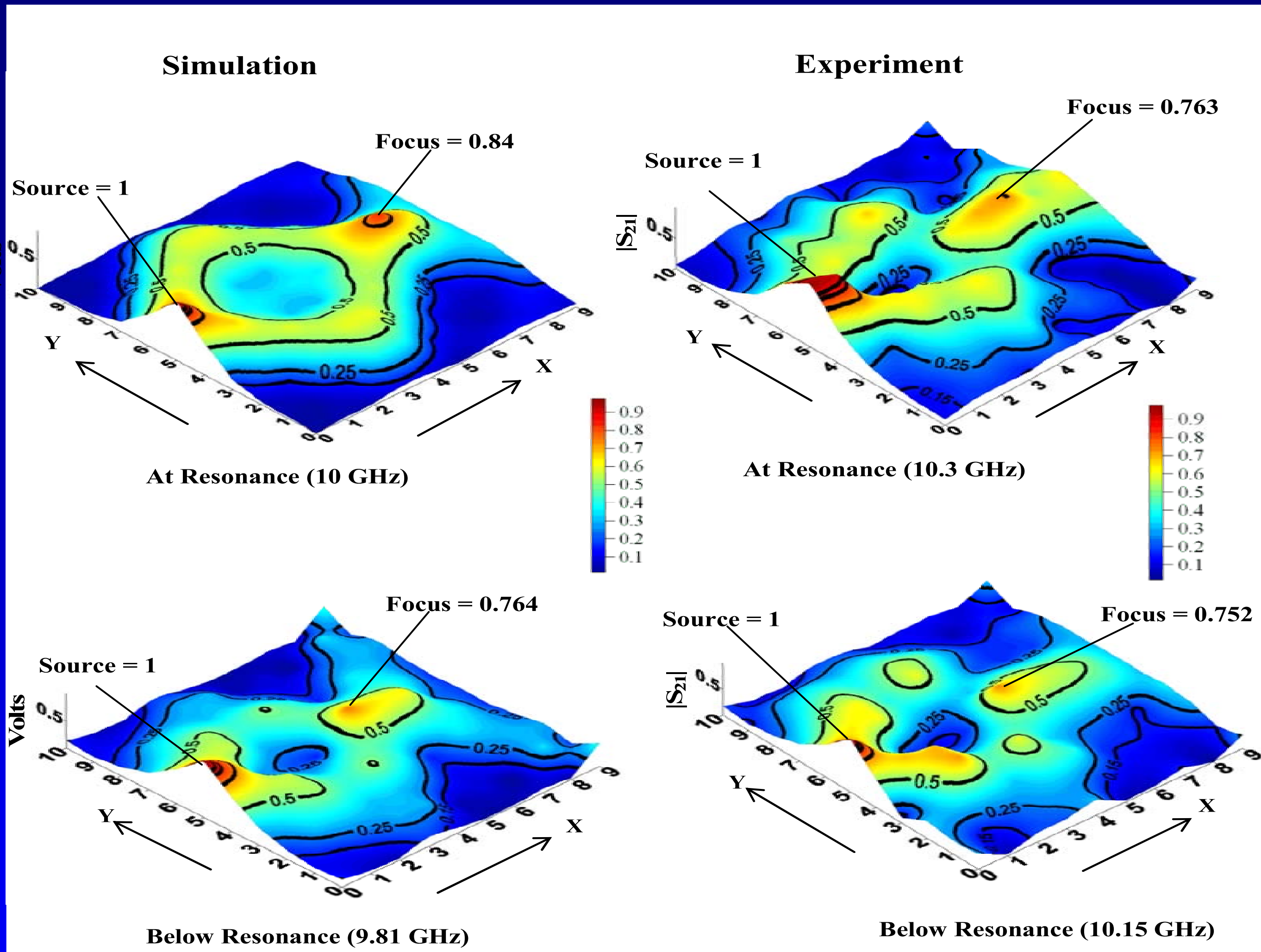

G.V. Eleftheriades and O.F. Siddiqui, "Negative refraction and focusing in hyperbolic transmission-line grids," *IEEE Trans. on Microwave Theory and Techniques,* vol. 53, *no. 1,* pp. 396- 403, Jan. 2005.

A DIPLEXER BASED ON NEGATIVE REFRACTION AND SPATIAL FILTERING

Photonic-Crystal Metamaterial

No lumped elements (chip or printed)

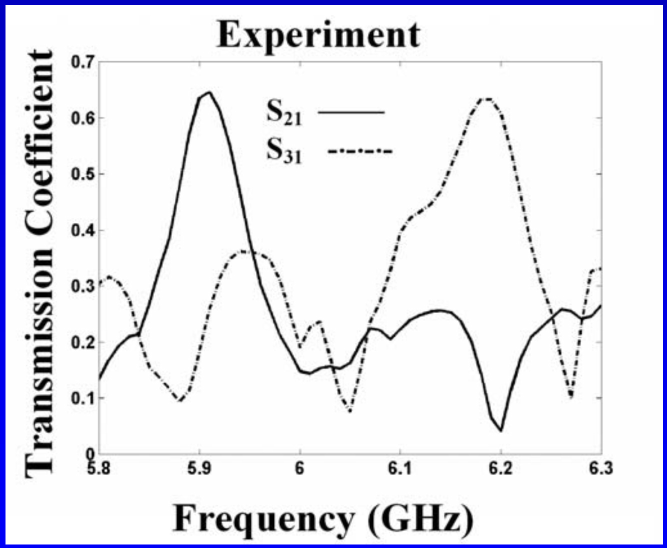

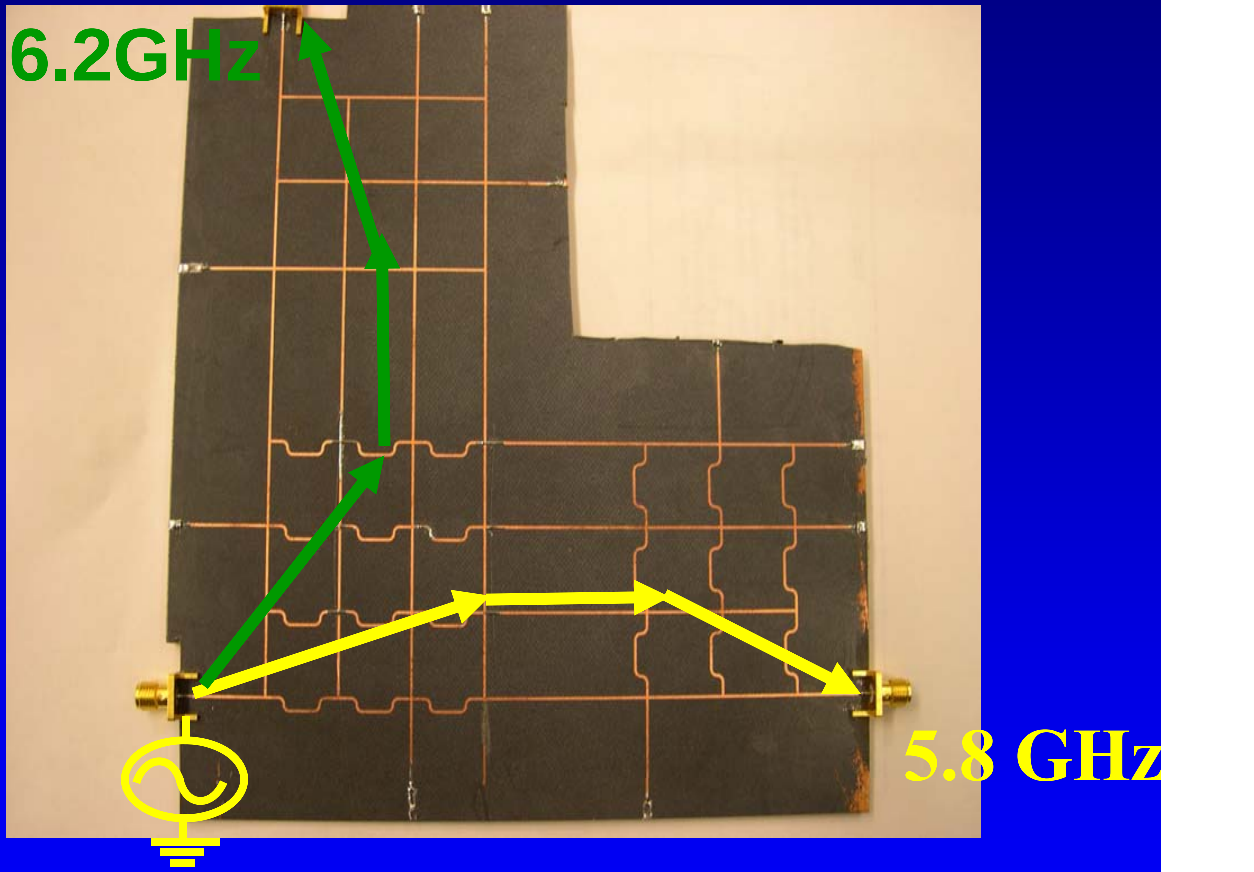

O.F. Siddiqui, and G.V. Eleftheriades, *Journal of Applied Physics,* 99, 083102, April 15, 2006.

A Shifted-Bean Approach to Sub-wavelength Focusing

Slots are closely spaced (lambda/10) and close to resonance

- The spot size is NOT sensitive to losses
- Simple to construct/frequency scalable structure
- Resonance enhances field transmission

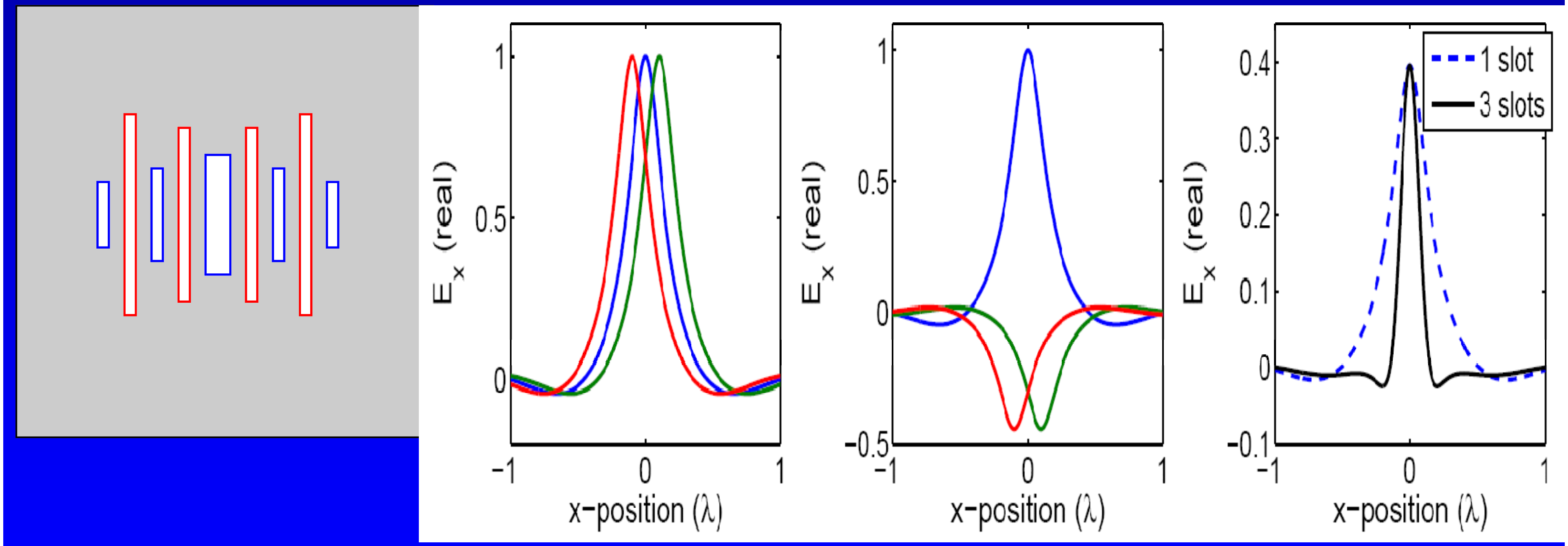

L. Markley, A.M.H. Wong, Y. Wang and G.V. Eleftheriades, "Spatially shifted beam approach to sub-wavelength focusing," *Physical Review Letters,* 101, 113901, Sept. 12, 2008.

Experimental Apparatus

5-slit Screen at $f = 10$GHz, $\lambda = 30$mm

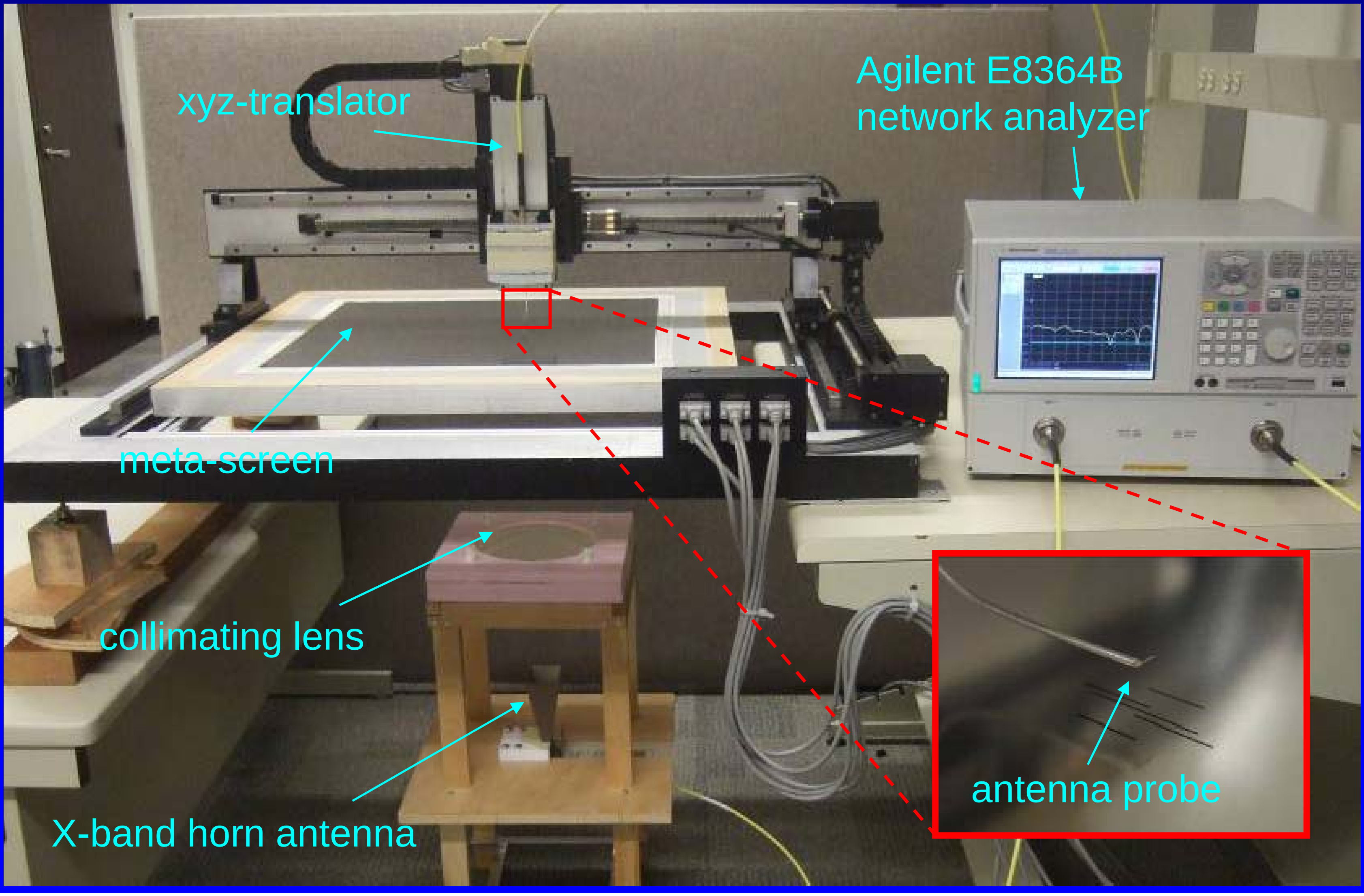

Experimental Results (2D Focusing)

- measurements taken 7.5 mm above the screen (0.25λ) at 10 GHz
  - 30mm by 30mm surface at 0.25mm increments shown at left in blue contours
- satellite slots were covered by copper tape and the single-slot pattern measured
  - FWHM contour shown in red
- beam width along the x-axis 0.271λ and along the z-axis is 0.385λ

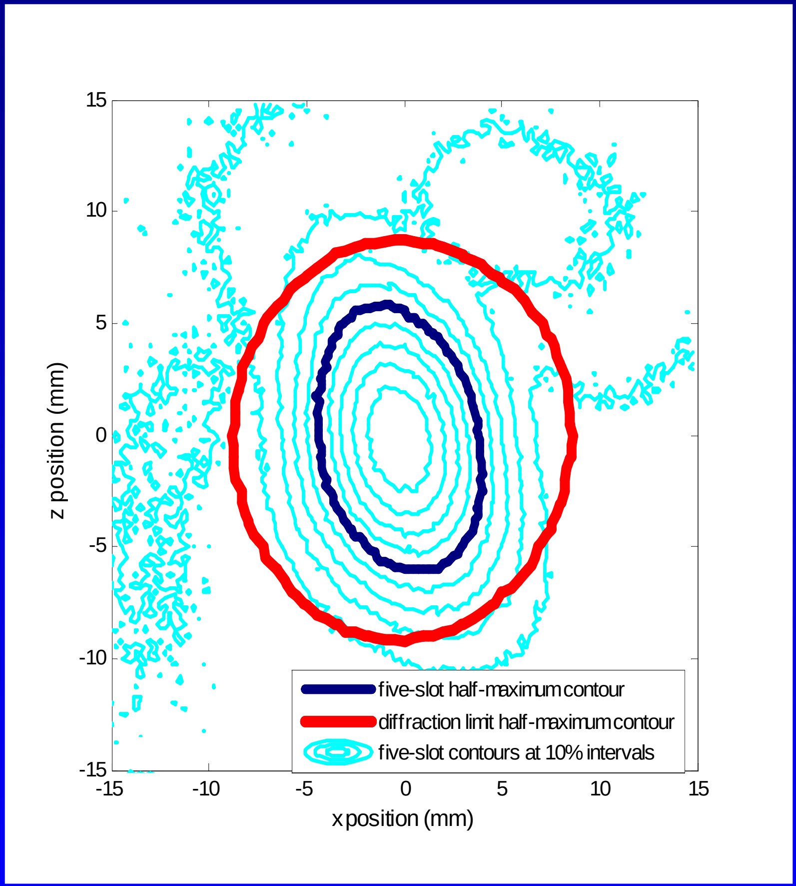

G.V. Eleftheriades and A.M.H. Wong, "Holography inspired screens for sub-wavelength focusing in the near field," *IEEE Microwave. Wireless Compon. Letters*, pp. 236-238, April. 2008.

Detecting Thru Reflection with Sub-wavelength Resolution

For the two washer case, the array probe clearly resolves them at a separation of 0.4λ @ 0.25 λ away (a single dipole probe cannot).

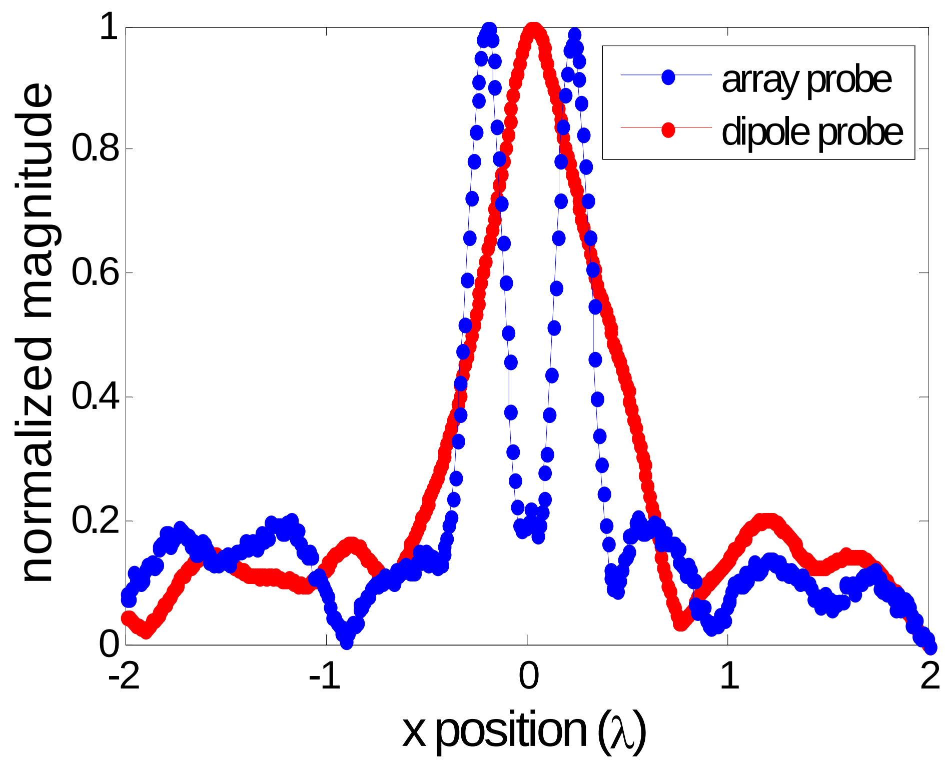

L. Markley and G.V. Eleftheriades, IEEE IMS, June 09, 2009 Boston.

EMERGING TRENDS AND APPLICATIONS

UNIQUE PROPERTIES CAN LEAD TO UNIQUE APPLICATIONS
(negative refraction, super-resolution, wavelength ~ freq, cloaking)

DIFFERENT PERSPECTIVE OF LOOKING AT THE WORLD!

RF/MICROWAVE PASSIVE COMPONENTS
SMALL ANTENNAS
ANTENNA BEAMFORMING
RCS MANAGEMENT/CLOAKING
MEDICAL IMAGING
TUNABLE AND ACTIVE METAMATERIAL STRUCTURES
EMI REDUCTION USING METAMATERIAL GROUNDS
THz COMPONENTS
BEYOND NRI METAMATERIALS

G.V. Eleftheriades, "EM Transmission-line metamaterials", *Materials Today*, vol. 12, pp. 30-41, March 2009 .